I-A METHANOL TO GASOLINE PROCESS

by

Sebastian Joseph

and

Yatish T. Shah

Chemical and Petroleum Engineering Department
University of Pittsburgh
Pittsburgh, PA 15261

CONTENTS

		Page
I-A	**METHANOL TO GASOLINE PROCESS**	I-1
	SUMMARY	I-5
	Introduction	I-6
	Methanol to Gasoline Process	I-8
	Reaction Mechanism	I-10
	Fluidized Bed Reactor	I-13
	Case Study	I-25
	Fixed Bed Reactor	I-29
	Case Study	I-41
	Comparison of Fixed and Fluidized Bed Reactors	I-45
	Conclusions	I-54
	Nomenclature	I-56
	References	I-58
	Appendix I-A	I-A-1

LIST OF FIGURES

		Page
I-A-1	Gasoline from Coal or Natural Gas via MTG.....	I-6
I-A-2	Schematic Representation of Fluidized Bed Reactor and Regenerator System.....	I-15
I-A-3	Representation of Fluid Bed Reactor According to the Model of Fryer and Potter.....	I-17
I-A-4	Typical Concentration Profiles of Reactants and Products in Fluidized Bed Reactor.....	I-27
I-A-5	Schematic Representation of Fixed Bed Reactor.....	I-30
I-A-6	Concentration Profiles of Reactant and Products in Fixed Bed Reactor.....	I-43
I-A-7	Product Distribution of Hydrocarbons in Fixed Bed.....	I-44
I-A-8	Temperature Profile in Fixed Bed Reactor.....	I-47
I-A-9	Conversion as a Function of WHSV for Fixed and Fluidized Bed Reactors.....	I-49
I-A-10	STY as a Function of WHSV for Fixed and Fluidized Bed Reactors.....	I-50
I-A-11	Selectivity to Olefins in Fixed and Fluidized Bed Reactors as a Function of WHSV.....	I-51
I-A-12	Selectivity to Olefins as a Function of Methanol Conversion in Fixed and Fluidized Beds.....	I-53

LIST OF TABLES

		Page
I-A-1	Heats of Reaction for Major Reaction Steps in Methanol Conversion to Hydrocarbons.....	I-9
I-A-2	Properties of Cracking Catalysts Used in Cold Flow Studies.....	I-22
I-A-3	Comparison of Experimental and Predicted Rise Velocities.....	I-23
I-A-4	Comparison of Experimental and Predicted Conversions.....	I-26
I-A-5	Experimental and Predicted Olefins Distribution, mol %.....	I-26
I-A-6	Effect of Bubble Diameter on Conversion.....	I-28
I-A-7	Effect of Temperature on Conversion.....	I-28
I-A-8	Reactions in the Kinetic Scheme of Mihail, et. al. (1983b).....	I-32
I-A-9	Comparison of Experimental and Predicted Results for Fixed Bed Reactors.....	I-41
I-A-10	Experimental and Predicted Results for PDU.....	I-42

SUMMARY

Two reactor types have been proposed for Mobil's Methanol to Gasoline process - Fluidized Bed and Fixed Bed Reactor. In this report, these two reactor systems were modeled and computer programs developed for the reactor models. The fluidized bed was modeled using the Fryer-Potter counter current backmixing model, while the fixed bed was modeled using a pseudo-homogeneous reactor model. Results from the computer simulations were compared with pilot plant data. Although the conversions were correctly predicted, the product distributions were different due to the unknown SiO_2/Al_2O_3 ratio of the MTG catalyst used in the pilot plant studies. A comparison of the two reactor types was carried out as regards conversion and selectivity to olefins. The comparison showed that at the same WHSV (Weight Hourly Space Velocity) the fixed bed reactor gave a higher conversion and better selectivity towards olefins than the fluidized bed.

Introduction

Mobil has developed a novel process for the conversion of methanol to high octane gasoline in excellent yields using a shape selective zeolite catalyst called ZSM-5 (Meisel et al. (1977)). The coupling of this methanol-to-gasoline (MTG) process with the well-established commercial technology for the conversion of coal (or any carbon source) to methanol provides a new route for the conversion of coal to gasoline (Figure I-A-1). The key element in the MTG process is the ZSM-5 zeolite catalyst. The pore structure of ZSM-5 consists of intersecting channels with diameters of about 6 A^{o} which are just large enough to produce hydrocarbons boiling in the gasoline range. Mobil has proposed two reactor systems for this process-fixed bed and fluidized bed. The first commercial plant for the MTG process is a 14,000 BPD gasoline plant in New Zealand, based on the fixed bed reactor concept (Penick et al. (1983), and Haggin (1985)).

The purpose of the present work is to model the two reactor systems that are used for the MTG process, namely, the fluidized bed reactor and the fixed bed reactor and to develop computer programs for these models. The simulation of these reactors can lead to an evaluation of reactor performance as well as validating kinetic mechanisms developed for the MTG reaction. The programs are written in a modular form in FORTRAN and the codes have been implemented on the University of Pittsburgh DEC System-1099 computer. The programs can be easily adapted to the ASPEN simulator by converting them into user models. Included in this report are the model development for the fluidized and fixed bed reactors, description of the numerical methods used to predict the performance of the units, source code of the programs, instructions for their use and a sample problem showing both the input data and the resulting output.

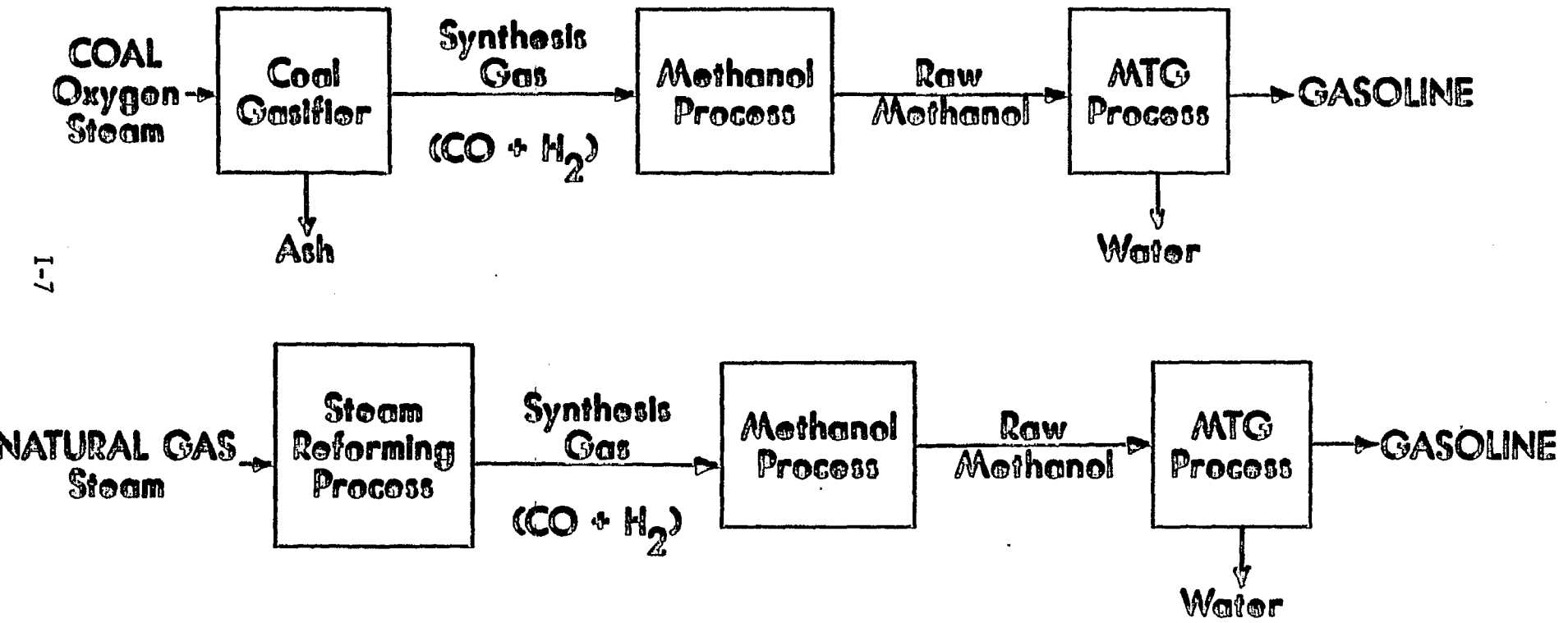

Figure I-A-1: Gasoline from coal or natural gas via MTG (from Penick et al., 1983).

Methanol to Gasoline Process

In the MTG process, methanol is converted to hydrocarbons and water. The process is highly selective and can be represented by the following overall reaction:

$$nCH_3OH \rightarrow \text{hydrocarbons} + nH_2O \qquad (1)$$

Quantitatively, 100 tons of methanol is converted to nearly 44 tons of hydrocarbons and 56 tons of water. The hydrocarbons produced contain 95% of the energy in the methanol feedstock; the exothermic heat of reaction contains the remaining energy.

The conversion of methanol to hydrocarbons over ZSM-5 can be represented by the following sequence of steps (Chang and Silvestri (1977)):

$$2CH_3OH \underset{+H_2O}{\overset{-H_2O}{\rightleftharpoons}} CH_3OCH_3$$

$$CH_3OCH_3 \xrightarrow{-H_2O} C_2\text{-}C_5 \text{ olefins}$$

$$C_2\text{-}C_5 \text{ olefins} \rightarrow \begin{matrix}\text{Paraffins}\\ \text{Aromatics}\\ \text{Cycloparaffins}\end{matrix}$$

The intial dehydration reaction is rapid and essentially at equilibrium over a wide range of conditions. Due to the selective nature of the ZSM-5 catalyst, no hydrocarbons above C_{10} are formed under MTG conditions.

The unique catalyst and reaction mechanisms impose several design constraints in the design of the reactor systems for the MTG process. These

include the highly exothermic nature of the reaction, the need for essentially complete methanol conversion, steam deactivation of the catalyst, the "band-aging" phenomenon, and durene formation.

a. Thermochemistry

The MTG reaction is highly exothermic and the heat of reaction is in the range 1510-1740 (kJ/kg of methanol) depending on the particular product distribution. This heat of reaction, if uncontrolled, would give an adiabatic temperature rise of about 600°C. The following table gives the heats of reaction for the major reaction steps in the conversion of methanol to hydrocarbons (Chang and Silvestri (1977)).

Table I-A-1: Heats of Reaction for Major Reaction Steps in Methanol Conversion to Hydrocarbons[@]

Reaction	$(-\Delta H^r)$ kcal	% of total heat of reaction
$CH_3OH \rightarrow \frac{1}{2} CH_3OCH_3 + \frac{1}{2} H_2O$	2.410	22.5
$\frac{1}{2} CH_3OCH_3 \rightarrow (CH_2)_{olefins} + \frac{1}{2} H_2O$	4.466	41.8
$(CH_2)_{olefins} \rightarrow (CH_2)_{hydrocarbons}$	3.814	35.7
$CH_3OH \rightarrow (CH_2)_{hydrocarbons} + H_2O$	10.69	100.0

[@]based on 1 gmole of methanol and t = 371°C

b. Complete Methanol Conversion

The major products of the MTG reaction are hydrocarbons and water. Hence, any unconverted methanol will dissolve into the water phase and recovery of this methanol would entail adding a distillation step to process the very dilute water phase. Thus, essentially complete conversion of methanol is sought.

c. Catalyst Deactivation

The ZSM-5 catalyst undergoes two types of aging which contribute to a gradual loss of catalyst activity. A reversible loss results from coke formed on the catalyst as a reaction product. The second type of deactivation results from one of the reaction products, steam. Low reactor temperatures and low partial pressures of water minimize the aging and favor a longer catalyst life.

d. Band-Aging

This phenomenon occurs only in fixed beds with fresh catalysts, where the reaction occurs over a relatively small zone in a fixed bed. This reaction front moves down the catalyst bed as the coke deposits first deactivate the front part of the bed. The use of a sufficient catalyst volume permits a fixed-bed design in which on-stream periods are long enough to avoid frequent regeneration of catalyst.

e. Durene Formation

Among the aromatic compounds formed in the MTG reaction is durene (1,2,4,5-tetramethyl-benzene). Durene has a relatively high freezing point of 79 ^{o}C. Gasoline obtained directly from the reactors could contain 4 to 7 wt% durene. These high concentrations of durene could lead to problems with solids build-up on carburetors during cold starts. Durene is mostly formed by alkylation of lower molecular weight aromatics with methanol. Low methanol partial pressures and high reaction temperatures tend to reduce the durene level.

Reaction Mechanism

Chang (1983) has discussed the various reaction mechanisms that have been postulated in the literature for the MTG process. Most of the models are based on the following assumptions:

(a) Methanol and Dimethyl ether (DME) are always at equilibrium and can be treated as a single kinetic species,

(b) Olefins can be treated as a single kinetic species,

(c) The sum of paraffins and aromatics can be treated as a single kinetic species.

Assumption (a) has been shown to be valid by the observation that over a wide range of conversions, the initial step of ether formation is much more rapid than the subsequent olefin-forming step and is essentially at equilibrium. Chen and Reagan (1979) discovered that the reaction was autocatalytic over ZSM-5. The following scheme was proposed:

$$A \rightarrow B$$

$$A+B \rightarrow B$$

$$B \rightarrow C$$

where

A = oxygenates (methanol + DME); B = olefins; C = paraffins + aromatics

Chang (1980) modified this scheme to account for the homologation of olefins.

$$A \rightarrow B$$

$$A+B \rightarrow C$$

$$B+C \rightarrow C$$

$$C \rightarrow D$$

where A = oxygenates; B = ($:CH_2$); C = olefins; D = paraffins + aromatics

Anthony (1981) pointed out an inconsistency in the derivation of the expression for the reaction rate for the above scheme. Futhermore, data at only one temperature was analyzed and hence extrapolation to other temperatures is not possible.

Recently, Mihail et al. (1983a, 1983b) have developed a detailed kinetic model for the conversion of methanol to olefins and hydrocarbons. The kinetic model for methanol to olefins is obtained for only one temperature. However, for the conversion of methanol-to hydrocarbons, kinetic parameters (Arrhenius frequency factor and activation energy) are obtained from non-isothermal operation. This detailed kinetic scheme involves 53 reaction steps and 37 kinetic species (including radical intermediates).

A kinetic scheme based on kinetic lumps has been proposed recently by Chang et al. (1984) based on the following mechanism:

$$A \xrightarrow{k_1} B \xrightarrow{k_2} C$$

where A = oxygenates; B = olefins; C = paraffins + aromatics

These lumps are defined on a water-free basis. The disappearance of oxygenates and olefins are assumed to be first-order. The kinetic parameters k_1 and k_2 were determined over a range of temperatures and SiO_2/Al_2O_3 ratios in the catalyst. For a SiO_2/Al_2O_3 ratio of ~ 450, they obtained:

$$k_1 = 1.09 \times 10^7 \exp\left(\frac{-10366}{T}\right) s^{-1}$$

$$k_2 = 0.98\ s^{-1}$$

The data for olefin disappearance (k_2) showed little or no temperature effect. The data of Chen and Reagan (1979) for k_1 is well correlated by the above expression for k_1.

a. Effect of Pressure

Chang et al. (1978) found that the main effect of increasing pressure in the MTG synthesis was to promote the formation of higher aromatics, especially durene and to increase gasoline yield. From their data, Chang et al. (1978) concluded that the formation of higher aromatics was not primarily a result of increased contact time but represented an intrinsic change in reaction selectivity with increased pressure. Liederman et al. (1978) took into account the inhibition effects caused by the adsorption of reactants and/or products with an increase in pressure by a simple expression of the type $(1/1+K_AP_A)$ where K_A is an adsorption constant and P_A is the sum of the partial pressure of methanol, dimethyl ether and water. They calculated K_A to be 1.5.

b. Effect of Zeolite SiO_2/Al_2O_3

Chang et al. (1984) studied the effect of temperature, pressure, contact time and catalyst Bronsted acidity on olefin selectivity and found that olefin formation could be decoupled from aromatization via a combination of high temperature and low catalyst acidity (high SiO_2/Al_2O_3 ratios). A similar observation regarding this effect of SiO_2/Al_2O_3 ratio has been observed by Kikuchi et. al. (1984).

Fluidized Bed Reactor

Though the New Zealand MTG plant was based on the fixed bed reactor concept, Mobil plans to use the fluidized bed reactor concept for future plants (Penick et al. (1983)). To this end, a 100 BPD pilot plant has been commissioned in West Germany (Flatow et al. (1984)).

Mobil initially carried out laboratory scale studies in a 4.13 cm diameter fluidized bed reactor (Voltz et al. (1976)). Later a 10.12 cm diameter fluidized bed was used for carrying out studies under cold flow and reactive conditions (Kam et al. (1978)). The erection of a 100 BPD, 60 cm diameter fluid bed has been achieved (Flatow et al. (1984)).

a Process Description

The process development unit (PDU) fluid bed reactor first built by Mobil consisted of a 4.12 cm diameter column with 5 zones which were heated by an electrical resistance furnance (Voltz and Wise (1976)). The total height of the unit was 73.6 cm. During operation, the charge stock and nitrogen carrier gas were pumped through a preheater coil where the charge was vaporized. The reaction occured in the dense fluid bed which contained four umbrella-shaped baffles to minimize gas by-passing. The next stage in the fluid bed development consisted of the following design features (Figure I-A-2).

- o 10.2 cm diameter by 762 cm high adiabatic dense fluid bed reactor.
- o External line for recirculating entrained catalyst to the reactor.
- o Intermittent regeneration of catalyst to maintain day-to-day steady state operation.

b. Fluidized Bed Reactor Model

Several models have been proposed in the literature for fluidized bed reactors. A review of these models is given by Yates (1983). Most models are based on the two-phase theory of fluidization which states that "all gas in excess of that necessary to just fluidize the bed passes through in the form of bubbles." The various models differ in their assumptions regarding the

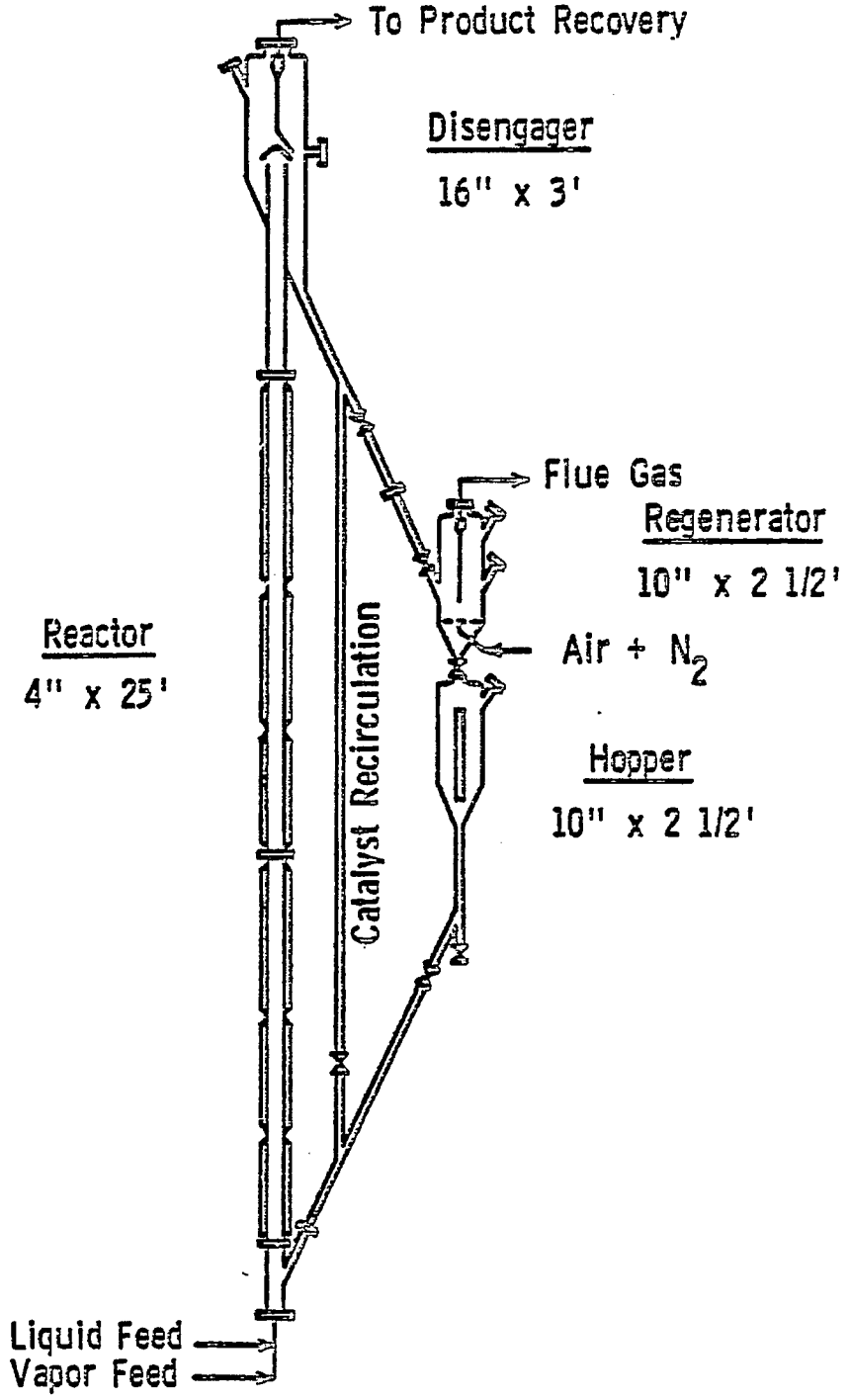

Figure I-A-2: Schematic representation of fluidized bed reactor and regenerator system.

exact nature of the phases (bubble, cloud-wake and emulsion) and degree of gas mixing in the phases. The model types can be divided into:

(i) simple or arbitrary models based on empirical correlations obtained with small scale equipment and

(ii) models based on bubble dynamics which describe reactor behavior in terms of the known physics and hydrodynamics of fluid beds.

For the present purposes of modeling, the countercurrent backmixing model of Fryer and Potter (1972), which is essentially an elaborate version of the Kunii-Levenspiel bubbling bed model (Kunii and Levenspiel (1968a, 1968b)) will be used. This model is described in the next section.

c. Countercurrent Backmixing Model of Fryer-Potter

The assumptions made in this model are as follows:

(i) Bubbles are of one size and are evenly distributed in the bed.

(ii) Each bubble drags along with it a wake of solids, creating a circulation of solids in the bed, with upflow behind bubbles and downflow in the rest of the emulsion.

(iii) The emulsion stays at minimum fluidizing conditions; thus the relative velocity of gas and solid remain unchanged.

(iv) Interphase gas exchange occurs in two stages: from bubble to cloud and from cloud to the particulate phase.

The model of Fryer and Potter (1972) is shown in Figure I-A-3. The superficial fluidizing gas velocity is:

$$U = U_{GB} + U_{GP} + U_{GC} \qquad (2)$$

Since bubble and cloud-wake rise together at the same absolute velocity

$$U_{GC} = f_w \varepsilon_{mf} U_{GB} \quad \text{.....(3)}$$

The backmixing model assumes that the relative velocity of gas to solids in the particulate phase is the same as at incipient fluidization, i.e.

$$\frac{U_{GP}}{[1-\varepsilon_B(1+f_w)]\varepsilon_{mf}} + \frac{U_{GB} f_w (1-\varepsilon_{mf})}{[1-\varepsilon_B(1+f_w)](1-\varepsilon_{mf})} = \frac{U_{mf}}{\varepsilon_{mf}} \quad \text{.....(4)}$$

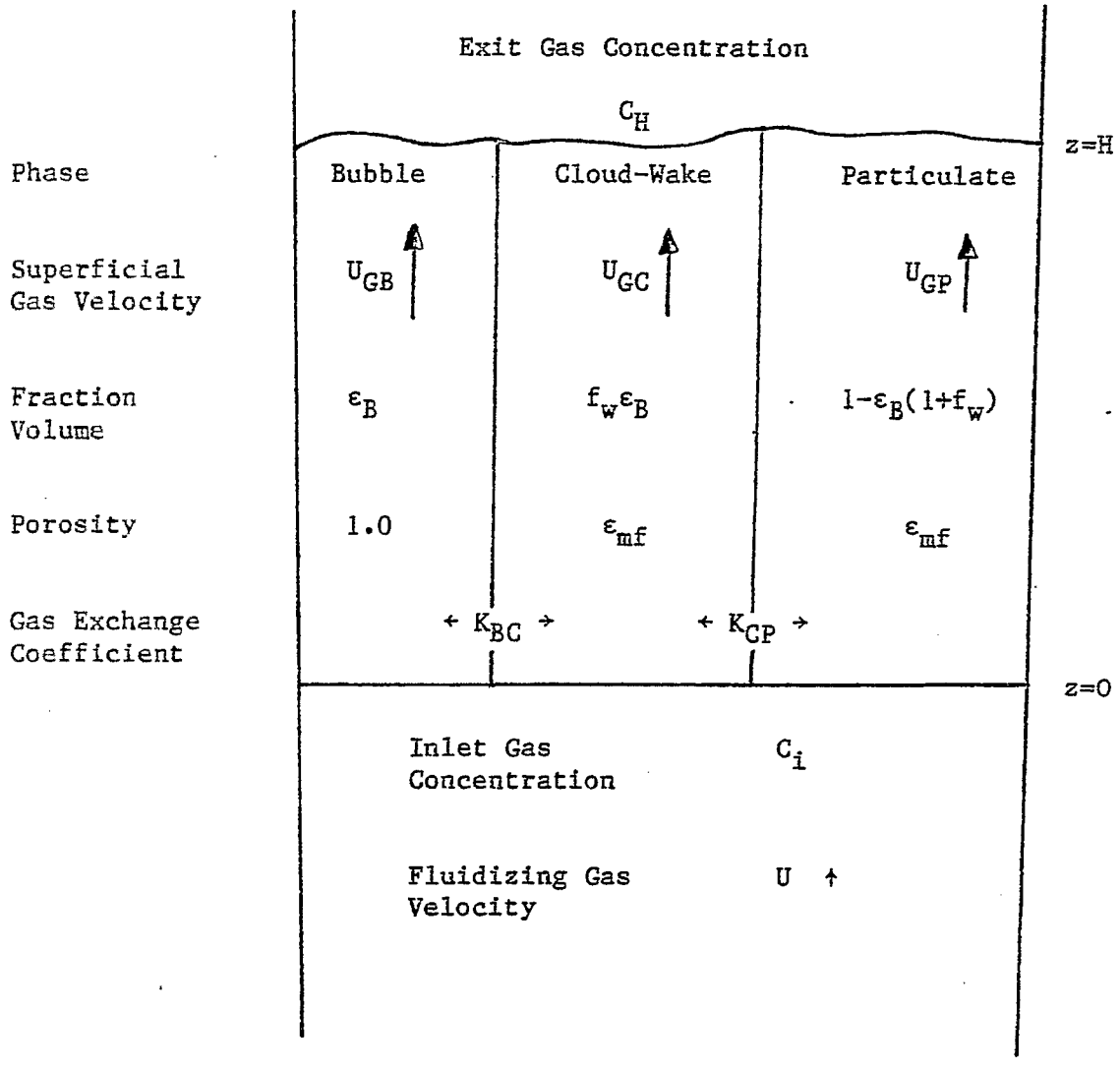

Figure I-A-3: Representation of Fluid Bed Reactor According to the Model of Fryer and Potter (1972).

Thus the superficial gas velocities in the bubble and particulate phases can be obtained from equations (2), (3) and (4) as:

$$U_{GB} = U - U_{mf}[1-\varepsilon_B(1+f_w)] \tag{5}$$

$$U_{GP} = U_{mf}[1-\varepsilon_B(1+f_w)]\ [1+\varepsilon_{mf}f_w] - Uf_w\varepsilon_{mf} \tag{6}$$

Backmixing of gas (i.e., negative U_{GP}) is predicted if U exceeds a critical value, U_{cr}, where:

$$\frac{U_{cr}}{U_{mf}} = [1 + \frac{1}{\varepsilon_{mf}f_w}]\ [1 - \varepsilon_B\ (1+f_w)] \tag{7}$$

The coefficients for gas exchange between bubble and cloud-wake phase and cloud-wake and particulate phase are given by Kunii and Levenspiel (1968b) as follows:

$$K_{BC} = 4.5\ (\frac{U_{mf}}{D_B}) + 5.85\ (\frac{g^{1/4}D_G^{1/2}}{D_B^{5/4}}) \tag{8}$$

$$K_{CP} = 6.78\ (\frac{\varepsilon_{mf}D_G u_A}{D_B^3})^{1/2} \tag{9}$$

The bubble rise velocity, u_A can be obtained from the following equation:

$$u_A = U-U_{mf}\ [1-\varepsilon_B(1+f_w)] + 0.71(gD_B)^{1/2} \tag{10}$$

and the bubble volume fraction is given by

$$\varepsilon_B = \frac{U_{GB}}{u_A} \tag{11}$$

The value of f_w is taken as approximately unity except that when $\varepsilon_B > 1/3$, f_w is reduced:

$$f_w = \frac{1-\varepsilon_B}{2\varepsilon_B} \tag{12}$$

This modification is introduced to ensure that the cloud-wake phase should never exceed the dense phase, i.e.:

$$\varepsilon_B f_w = 1-\varepsilon_B\ (1+f_w) \tag{13}$$

The model equations are developed for steady-state, irreversible, constant-volume gas phase reactions of the first order. The contact of reactant with the very small amount of solids which may be dispersed in the bubble phase is neglected. The material balances on reactant gas in the bubble, cloud-wake and particulate phases, respectively, are:

$$\frac{-dC_B}{dz} = \frac{K_{BC}(C_B-C_C)\varepsilon_B}{U_{GB}} \tag{14}$$

$$\frac{-dC_C}{dz} = \frac{K_{CP}(C_C-C_P)\varepsilon_B+K_{BC}(C_C-C_B)\varepsilon_B+kC_C f_w \varepsilon_B}{U_{GC}} \tag{15}$$

$$\frac{-dC_P}{dz} = \frac{K_{CP}(C_P-C_C)\varepsilon_B+kC_P[1-\varepsilon_B(1+f_w)]}{U_{GP}} \tag{16}$$

The boundary conditions are written for backmixing conditions (i.e., when U is sufficiently large to cause downflow of particulate gas. From equation (7) this is seen to occur for $U > 3\text{-}11U_{mf}$, which in most industrial situations is valid).

(a) at the distributor level (z=0) all bubble gas is considered to derive from the incoming gas

$$C_B = C_i \tag{17}$$

The remainder of the incoming gas combines with downflowing particulate phase gas to constitute the cloud-wake gas

$$-U_{GP}\, C_p + (U-U_{GB})\, C_i = U_{GC}\, C_C \tag{18}$$

(b) At the top of the bed (z=H) gas leaving the bed is considered to be made up of all the bubble gas and some cloud-wake gas with the remainder of the cloud-wake gas providing the downflowing gas in the particulate phase

$$C_P = C_C \tag{19}$$

The required expression for the exit gas concentration is

$$UC_H = U_{GB}\, C_B + (U - U_{GB})\, C_C \tag{20}$$

An analytical solution to the above boundary value problem has been provided by Fryer and Potter (1972). As stated earlier, this model is basically an extension of the Kunii-Levespiel bubbling bed model and the model equations for the bubbling bed model can be achieved by simply ignoring the throughflow of gas in the cloud-wake and particulate phases (i.e. $U_{GC} = 0$, $U_{GP} = 0$). Note

that some authors have mistakenly assumed the resulting expressions to imply completely mixed cloud-wake and particulate phase gas, which is obviously not true.

d. Slugging in Fluidized Beds

Slugging occurs in deep fluidized beds of high aspect ratio where the continuation of bubble coalescence leads eventually to the formation of bubbles whose diameter is equal to that of the bed itself. Such bubbles are called slugs and their hydrodynamic properties are different from those of freely moving bubbles. Stewart and Davidson (1967) have proposed a criterion to determine the onset of slugging. The following equation gives the minimum excess gas velocity at which slugs will form in a tube of diameter D_T.

$$(U-U_{mf}) = 0.07\ (gD_T)^{1/2} \qquad (21)$$

From cold flow studies in a 10.12 cm diameter fluidized bed, Kam et al. (1978) determined U_{mf} to be 0.15 cm/sec for a particle size range of 70-75 μm. From equation (21) the minimum excess gas velocity to cause slugging is calculated to be 7.1 cm/sec. In view of the fact that gas velocities in the range 30-60 cm/sec were used under reacting conditions, it seems that slugging would definitely occur in the fluidized bed reactor. However, Kam et al. (1978) found from their cold flow studies that, with two different catalyst types, D10 and CBZ-1, slugging in the bed was less pronounced with D10 compared to CBZ-1. The properties of these two catalysts are given in Table I-A-2.

Table I-A-2: Properties of Cracking Catalysts Used in Cold Flow Studies (Kam et al. (1978)).

Physical Analysis	CBZ-1	D10
Surface Area, m^2/gm	290	335
Pore Volume, cc/gm	0.577	0.975
Packed Density, gm/cc	0.64	0.63
Loosely Packed Density, gm/cc	0.53	0.47
Particle Density, gm/cc	1.035	0.73
Real Density, gm/cc	2.569	2.53

Furthermore, contrary to what was observed with CBZ-1, slugging with D10 catalyst decreased as the superficial gas velocity increased. They explained this unusual phenomenon on the basis of the maximum stable bubble size that could occur in the column. For D10, this size was determined to be 7.6 cm, while that for CBZ-1 was 12.1 cm. The maximum stable bubble size for D10 is less than the reactor diameter (10.12 cm) while that for CBZ-1 is larger. Hence, less slugging was observed with D10 compared to CBZ-1. Another indirect proof to show that slugging was absent comes from the bubble velocity measurements carried out by Kam et al. (1978). The rise velocity of continuously generated slugs is given by

$$U_{SA} = U - U_{mf} + 0.35\ (gD_T)^{1/2} \qquad (22)$$

Table I-A-3 shows the experimental values of Kam et al. (1978) and rise velocities predicted by equation (22).

Table I-A-3: Comparison of Experimental and Predicted Rise Velocities

U, cm/sec	Experimental, cm/sec	Predicted, cm/sec
15.2	56.1	49.9
21.3	84.1	56.0
42.7	167.9	77.4

From Table I-A-3, it is seen that equation (22) grossly underpredicts the rise velocities. It is known that slugs rise more slowly than bubbles of equal volume. Hence, in view of the fact that the Mobil catalyst used for the MTG process closely resembles D10 rather than CBZ-1, it is assumed that slugging is absent in the fluidized bed reactor and the backmixing model of Fryer and Potter is used for modeling the reactor.

e. Model Assumptions

The following assumptions are made in the development of the reactor model:

i) The temperature is constant along the length of the reactor. Even though the reactor was operated in an adiabatic manner, a very uniform temperature profile was obtained during the pilot plant operation (Kam et al. (1978)). Hence, this is a reasonable assumption.

ii) Though there is a slight expansion of the gas phase (about 20%), the superficial gas velocity is assumed to remain constant along the length of the reactor.

iii) The mass transfer coefficients for all species can be taken to be equal (Levenspiel et al. (1978)).

iv) The bubble diameter, D_B, is assumed to be equal to the maximum stable bubble size that can be achieved in the fluidized bed.

f. Input Parameters

To solve the model equations for the countercurrent backmixing model, the following parameters need to be known:

Solid particles	U_{mf}, ε_{mf}
Gas	D_G
Operating Parameters	U, H, d_t
Kinetic Data	k
Hydrodynamic parameter	D_B

The velocity at minimum fluidization conditions, U_{mf}, has been reported to be 0.15 cm/sec for the MTG catalyst (Kam and Lee (1978)). The voidage at minimum fluidization, ε_{mf}, was calculated from the following equation

$$\varepsilon_{mf} = 1 - \frac{\rho_{fL}}{\rho_p}$$

where ρ_{fL} = density of fluidized bed at minimum fluidizing conditions, 0.224 gm/cc

ρ_p = density of catalyst particle, 0.481 gm/cc

Hence, ε_{mf} is calculated to be 0.533.

The gas phase diffusivity, D_G, was calculated by means of the Chapman-Enskog formula for a binary gas mixture.

$$D_{AB} = 0.0018583 \frac{T^{3/2} (1/M_A + 1/M_B)^{1/2}}{p_t \sigma^2_{AB} \Omega_{AB}}$$

where D_{AB} = bulk diffusivity, cm^2/s

T = temperature, K

M_A, M_B = molecular weights of gases A & B

p_t = total pressure of the gas mixture, atm

σ_{AB}, ε_{AB} = constants in the Lennard-Jones potential-energy function for the molecular pair AB

Ω_{AB} = collision integral

Thus, D_G was calculated to be 0.18 cm^2/sec. Fryer and Potter (1972) made an extensive survey of the effect of the variables D_G, ε_{mf}, f_w and H_{mf} in the ranges of values: 0.1 to 1.0 cm^2/sec, 0.4 to 0.6, 0.5 to 1.0 and 25 to 200 cm respectively, and found their effect small in comparison with k, D_B, U_{mf} and U. Hence, the estimation of D_G is not very critical.

The operating parameters, U, H and d_t were taken from the Mobil report (Kam and Lee (1978)). The kinetic model of Chang et al. (1984) was used and the kinetic data were obtained from that paper. The bubble diameter D_B is an extremely critical parameter in these calculations and it was taken to be the maximum stable bubble size (7.5 cm).

g. Method of Solution

Even though the kinetic expressions are first-order, the model equations are solved numerically so that even non-linear rate expressions can be included later, if so desired. The model equations (14), (15) and (16) together with the boundary conditions, (17), (18) and (19) constitute a boundary value problem. This boundary value problem is solved using the software package COLSYS (Ascher et al. (1981)).

Case Study

Simulations of the fluidized bed were performed for various experimental runs found in the report of Kam and Lee (1978). The following table compares the experimental methanol conversions and those predicted from the Fryer-Potter model.

Table I-A-4: Comparison of Experimental and Predicted Conversions

Run No.@	U cm/s	Experimental Conversion, %	Predicted Conversion, %
CT-231-1-2	39.23	100.0	99.7
CT-231-1-11	47.28	99.42	99.28
CT-231-1-17	25.88	99.98	99.92

@From the appendix of the report by Kam and Lee (1978)

As can be seen, the conversions predicted by Fryer and Potter's model are in good agreement with the experimental conversions. The reaction model that is used here is a "lumped" kinetic model and hence the entire product distribution cannot be obtained. Only selectivities of "olefins" and "paraffins and aromatics" can be presently obtained. The concentration profiles of the various species are shown in Figure I-A-4. The following table shows the experimental and predicted olefins distribution.

Table I-A-5: Experimental and Predicted Olefins Distribution, mol %

Run No.	Experimental	Predicted
CT-231-2-62	29.44	1.5

The reason for the large discrepancy between experimental and predicted olefins selectivity is probably due to the nature of the catalysts used. As stated earlier, the SiO_2/Al_2O_3 ratio in the MTG catalyst can have a significant influence on the product distribution.

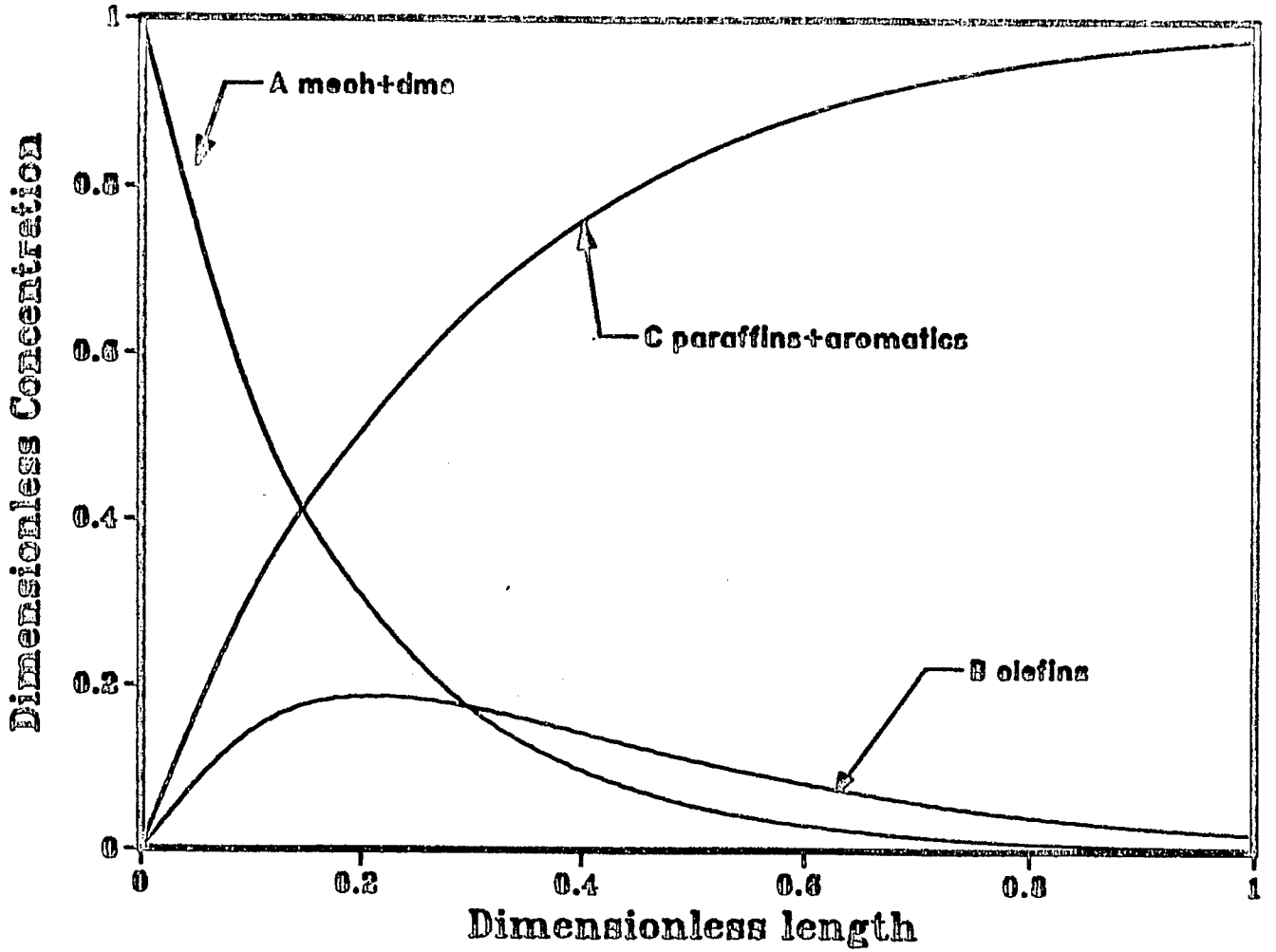

Figure I-A-4: Typical concentration profiles of reactants and products in fluidized bed reactor (WHSV = 1.1, T = 672.6K, P = 2.7 atm).

The bubble diameter is an extremely critical parameter in the countercurrent backmixing model and the following table shows the effect of bubble diameter on conversion.

Table I-A-6: Effect of Bubble Diameter on Conversion.
Run No. CT-231-1-2

D_B, cm	Conversion, %
7.5	99.7
8.5	99.4
10.2	98.5

A bubble size of 10.12 cm indicates that the bubble is a slug and theoretically, the countercurrent backmixing model of Fryer and Potter cannot be used to model the fluidized bed since the hydrodynamic properties of slugs are different from those of bubbles. Slugging bed models like those of Raghuraman and Potter (1978) or Yates and Gregoire (1980) would be the appropriate models to use and they would predict conversions lower than those indicated in Table I-A-6. The effect of temperature on conversion is shown in Table I-A-7. The conversion increases with an increase in temperature.

Table I-A-7: Effect of Temperature on Conversion

(U = 39.23 cm/s)

Temperature, ^oF	Conversion, %
650	95.84
700	98.94
762	99.70

Fixed Bed Reactor

a. Process Description

In the fixed bed process, two adiabatic reactors are used in series (Figure I-A-5). In the first reactor, methanol is partially dehydrated to an equilibrium mixture of methanol, dimethyl ether and water over a dehydration catalyst.

$$2CH_3OH \rightleftharpoons (CH_3)_2O + H_2O$$

This reaction is thermodynamically limited and does not go to completion. The effluent from the first reactor containing a near equilibrium mixture of methanol, dimethyl ether and water is fed to the second reactor where methanol and dimethyl ether are converted to hydrocarbons and water over a zeolite catalyst. Light gases are recycled to the second reactor to reduce the adiabatic temperature rise. The heat of reaction is removed from the product and recycle gases downstream to the reactor.

b. Fixed Bed Reactor Modeling

In modeling the fluidized bed, the lumped kinetic model of Chang et al. (1984) was used for the MTG reaction. This model was used since the temperature in the fluidized bed was uniform despite the adiabatic mode of operation and the heat balance was not required in modeling the fluidized bed. However, there is a significant temperature rise in the fixed bed reactor and hence the heat balance equation has to be included in the reactor model equations to model the temperature rise in the bed. The heat of reaction is one of the key terms that appears in the heat balance equation. Since the MTG reaction consists of many parallel and consecutive steps, it is not possible to assign a fixed value for the overall heat of reaction. Global

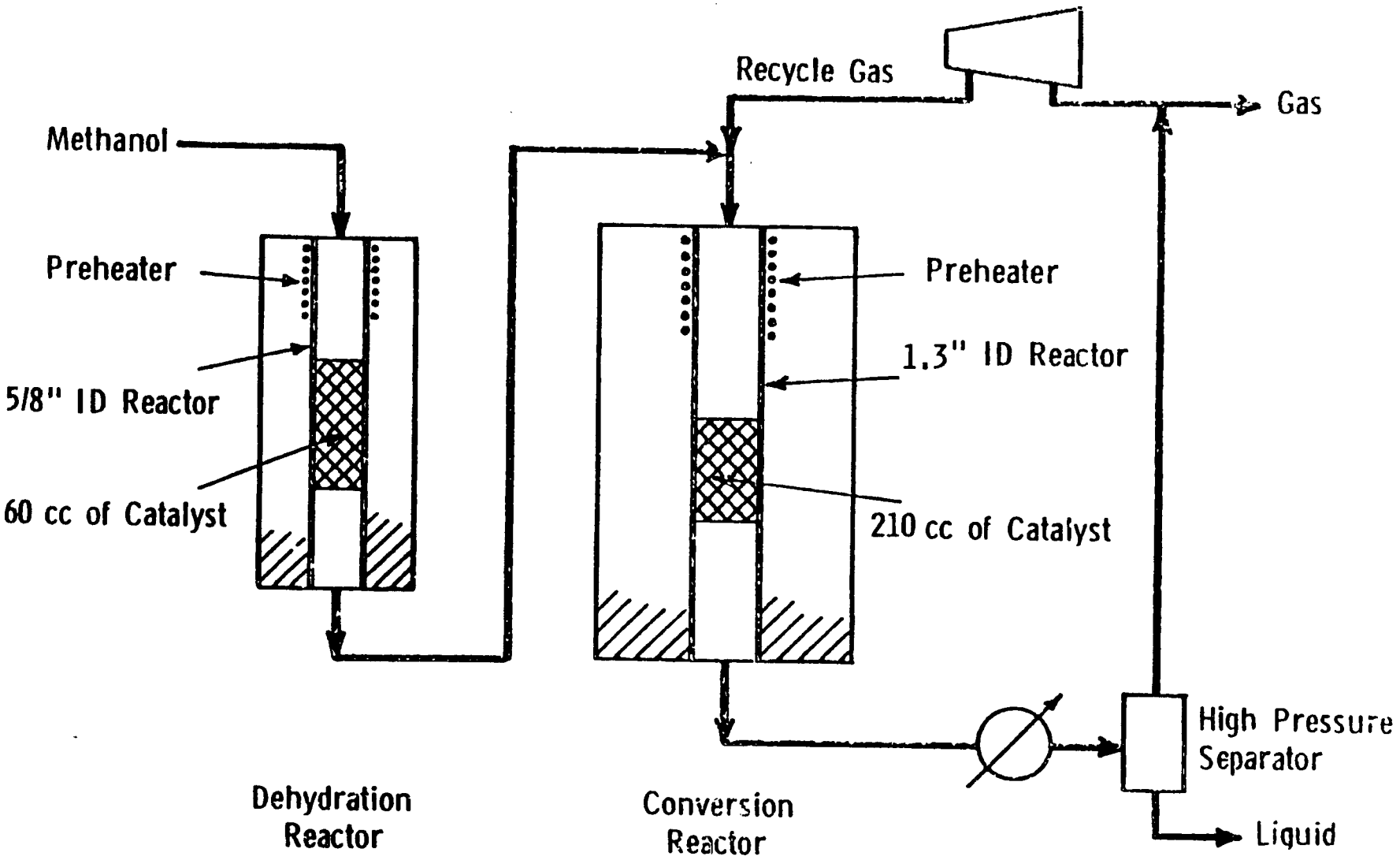

Figure I-A-5: Schematic representation of fixed bed reactor.

values of the heat of reaction will not lead to a satisfactory fit of the temperature profile. Hence, a rigorous design of the fixed bed requires a detailed reaction scheme. Such a detailed scheme would lead to a set of continuity equations for the various species which would directly predict the product distribution and the effect of temperature. Furthermore, the overall heat of reaction would be correctly calculated from the heats of reaction for the individual reactions, at all stages of conversion. As stated in the section on reaction mechanism, Mihail et al. (1983b) have developed a detailed kinetic model for the MTG reaction. Their model is as follows: the dimethyl ether at equilibrium with methanol, generates carbene; the carbene attacks the oxygenates giving light olefins, which then form higher olefins. The olefins, through carbenium ions form aromatics and paraffins. The various steps that are involved in the mechanism are outlined in Table I-A-8. This kinetic model was not used for the fluidized bed reactor model since the use of this model would lead to a set of 111 (37 species x 3 phases) non-linear differential equations which are essentially stiff in nature and constitute a boundary value problem. Computational time as well as memory requirements for this problem would be large and hence the lumped kinetic model was adopted for the fluidized bed model.

c. Dehydration Reactor

As shown in Figure I-A-5, the PDU consisted of a dehydration reactor, where methanol is converted to an equilibrium mixture of methanol, dimethyl ether and water. This reactor is also operated in an adiabatic manner. Equilibrium methanol conversions and adiabatic reactor exit temperatures as functions of reactor inlet temperature have been calculated by Chang et al. (1978). Their results can be correlated by the following expressions:

Table I-A-8: Reactions in the kinetic scheme of Mihail et al. (1983b)

I). Methanol reactions

1). $CH_3OH \rightarrow CO + 2H_2$

2). $2CH_3OH \rightleftarrows CH_3OCH_3 + H_2O$

3). $CH_3OCH_3 \rightarrow 2{:}CH_2 + H_2O$

II). Light olefins formation from carbene and oxygenates:

4). $:CH_2 + CH_3OH \rightarrow C_2H_4 + H_2O$

5). $:CH_2 + CH_3OCH_3 \rightarrow C_2H_4 + CH_3OH$

6). $:CH_2 + CH_3OCH_3 \rightarrow C_3H_6 + H_2O$

III). Higher olefins formation from carbene and light olefins:

7). $:CH_2 + C_2H_4 \rightarrow C_3H_6$

8). $:CH_2 + C_3H_6 \rightarrow C_4H_8$

9). $:CH_2 + C_4H_8 \rightarrow C_5H_{10}$

10). $:CH_2 + C_5H_{10} \rightarrow C_6H_{12}$

11). $:CH_2 + C_6H_{12} \rightarrow C_7H_{14}$

IV). Methane formation from carbene and hydrogen:

12). $:CH_2 + H_2 \rightarrow CH_4$

V). Carbenium ions formation from olefins:

13). $C_2H_4 \xrightarrow[-A^-]{+A^-H^+} C_2^+H_5$

14). $C_3H_6 \xrightarrow[-A^-]{+A^-H^+} C_3^+H_7$

Table I-A-8 (continued)

14). C_3H_6 $\overset{+A^-H^+}{\underset{-A^-}{\rightleftharpoons}}$ $C_3^+H_7$

15). C_4H_8 $\overset{+A^-H^+}{\underset{-A^-}{\rightleftharpoons}}$ $C_4^+H_9$

16). C_5H_{10} $\overset{+A^-H^+}{\underset{-A^-}{\rightleftharpoons}}$ $C_5^+H_{11}$

VI). Carbenium ions attack on light olefins giving higher olefins (oligomerization)

17). $C_3^+H_7 + C_3H_6$ $\overset{+A^-}{\underset{-A^-H^+}{\rightleftharpoons}}$ C_6H_{12}

18). $C_4^+H_9 + C_2H_4$ $\overset{+A^-}{\underset{-A^-H^+}{\rightleftharpoons}}$ C_6H_{12}

19). $C_4^+H_9 + C_3H_6$ $\overset{+A^-}{\underset{-A^-H^+}{\rightleftharpoons}}$ C_7H_{14}

20). $C_5^+H_{11} + C_2H_4$ $\overset{+A^-}{\underset{-A^-H^+}{\rightleftharpoons}}$ C_7H_{14}

VII). Carbenium ions attack on higher olefins giving paraffins and dienes:

21). $C_2^+H_5 + C_6H_{12}$ $\overset{+A^-}{\underset{-A^-H^+}{\rightleftharpoons}}$ $C_2H_6 + C_6H_{10}$

22). $C_2^+H_5 + C_7H_{14}$ $\overset{+A^-}{\underset{-A^-H^+}{\rightleftharpoons}}$ $C_2H_6 + C_7H_{12}$

23). $C_3^+H_7 + C_6H_{12}$ $\overset{+A^-}{\underset{-A^-H^+}{\rightleftharpoons}}$ $C_3H_8 + C_6H_{10}$

Table I-A-8 (continued)

24). $C_3^+H_7 + C_7H_{14} \rightleftarrows^{+A^-}_{-A^-H^+} C_3H_8 + C_7H_{12}$

25). $C_4^+H_9 + C_6H_{12} \rightleftarrows^{+A^-}_{-A^-H^+} C_4H_{10} + C_6H_{10}$

26). $C_4^+H_9 + C_7H_{14} \rightleftarrows^{+A^-}_{-A^-H^+} C_4H_{10} + C_7H_{12}$

27). $C_5^+H_{11} + C_6H_{12} \rightleftarrows^{+A^-}_{-A^-H^+} C_5H_{12} + C_6H_{10}$

28). $C_5^+H_{11} + C_7H_{14} \rightleftarrows^{+A^-}_{-A^-H^+} C_5H_{12} + C_7H_{12}$

VIII). Carbenium ions attack on dienes giving paraffins and cyclodienes:

29). $C_3^+H_7 + C_6H_{10} \rightleftarrows^{+A^-}_{-A^-H^+} C_6H_8 + C_3H_8$

30). $C_3^+H_7 + C_7H_{12} \rightleftarrows^{+A^-}_{-A^-H^+} C_7H_{10} + C_3H_8$

31). $C_4^+H_9 + C_6H_{10} \rightleftarrows^{+A^-}_{-A^-H^+} C_6H_8 + C_4H_{10}$

32). $C_4^+H_9 + C_7H_{12} \rightleftarrows^{+A^-}_{-A^-H^+} C_7H_{10} + C_4H_{10}$

33). $C_5^+H_{11} + C_6H_{10} \rightleftarrows^{+A^-}_{-A^-H^+} C_6H_8 + C_5H_{12}$

34). $C_5^+H_{11} + C_7H_{12} \rightleftarrows^{+A^-}_{-A^-H^+} C_7H_{10} + C_5H_{12}$

Table I-A-8 (continued)

IX). Carbenium ions attack on cyclodienes giving paraffins and aromatics:

35). $C_3^+H_7 + C_6H_8 \overset{+A^-}{\underset{-A^-H^+}{\rightleftharpoons}} C_6H_6 + C_3H_8$

36). $C_3^+H_7 + C_7H_{10} \overset{+A^-}{\underset{-A^-H^+}{\rightleftharpoons}} C_7H_8 + C_3H_8$

37). $C_4^+H_9 + C_6H_8 \overset{+A^-}{\underset{-A^-H^+}{\rightleftharpoons}} C_6H_6 + C_4H_{10}$

38). $C_4^+H_9 + C_7H_{10} \overset{+A^-}{\underset{-A^-H^+}{\rightleftharpoons}} C_7H_8 + C_4H_{10}$

39). $C_5^+H_{11} + C_6H_8 \overset{+A^-}{\underset{-A^-H^+}{\rightleftharpoons}} C_6H_6 + C_5H_{12}$

40). $C_5^+H_{11} + C_7H_{10} \overset{+A^-}{\underset{-A^-H^+}{\rightleftharpoons}} C_7H_8 + C_5H_{12}$

X). Aromatics condensation:

41). $2C_6H_6 \rightarrow C_{10}H_8 + C_2H_4$

42). $2C_6H_6 \rightarrow C_9H_8 + C_2H_4 + C$

Table I-A-8 (continued)

XI). Aromatics alkylation:

43). $CH_3OH + C_6H_6 \rightarrow C_7H_8 + H_2O$

44). $CH_3OH + C_7H_8 \rightarrow C_8H_{10} + H_2O$

45). $CH_3OH + C_8H_{10} \rightarrow C_9H_{12} + H_2O$

46). $CH_3OH + C_9H_{12} \rightarrow C_{10}H_{14} + H_2O$

47). $CH_3OH + C_{10}H_{14} \rightarrow C_{11}H_{16} + H_2O$

48). $CH_3OH + C_{11}H_{16} \rightarrow C_{12}H_{18} + H_2O$

49). $CH_3OH + C_{10}H_8 \rightarrow C_{11}H_{10} + H_2O$

50). $CH_3OH + C_{11}H_{10} \rightarrow C_{12}H_{12} + H_2O$

XII). Paraffins demethanization:

51). $C_5H_{12} \rightarrow C_4H_8 + CH_4$

52). $C_4H_{10} \rightarrow C_3H_6 + CH_4$

53). $C_3H_8 \rightarrow C_2H_4 + CH_4$

Feed	Pure Methanol	Crude Methanol (16 wt % water)
Equilibrium Conversion (%)	$-0.0315T^{*} + 99.788$	$-0.042T + 101.80$
Exit Temperature under Adiabatic Conditions (K)	$0.8165T + 225.14$	$0.833T + 193.62$

*T is in degrees Kelvin, and is the inlet temperature to the dehydration reactor.

d. Model Assumptions

The following assumptions are made in the development of the fixed bed reactor model:

i) the gas phase is assumed to be in plug flow. Since the L/D ratio for the fixed bed is greater than 7, this is a reasonable assumption.

ii) Since the kinetic parameters for the reaction scheme of Mihail et al. (1983b) were obtained adopting a pseudohomogeneous model for the reactor, the same reactor model is used in the present case i.e. no distinction is made between the fluid and solid temperature. This model assumes diffusional resistances and intraparticle resistances to be negligible. This assumption is quite restrictive and it has been made due to the absence of any experimental data regarding catalyst particle size and conversion. For the dehydration reaction of methanol, Swabb and Gates (1972) found that the effectiveness factor decreased from 0.93 to 0.62 as the mean catalyst (H-mordenite crystallites) pore length increased from 5.9 to 16.6 μ. In view of the fact that the catalyst particle sizes are not reported in the MTG experimental studies, this assumption of negligible intraparticle diffusion had to be made.

iii) An average pressure is used in the calculations since in most cases the pressure drop in a fixed bed reactor is relatively small (Froment and Bischoff (1979)).

e. Model Equations

Simulating the fixed bed reactor requires the following set of continuity equations for the components to be integrated, together with the heat balance equation.

$$\frac{dF_j}{dz} = R_j \frac{\pi d_t^2}{4} = \left(\sum_{i=1}^{NR} \alpha_{ij} r_i\right) \frac{\pi d_t^2}{4} \qquad j=1, NS \qquad (23)$$

where NR = number of reactions

NS = number of species

$$\frac{dT}{dz} = \frac{1}{\sum_{j=1}^{NS} F_j C_{pj}} \left\{\frac{\pi d_t^2}{4} \sum_{i=1}^{NR} (-\Delta H_i) r_i + q(z)\pi d_t\right\} \qquad (24)$$

Here, $$r_i = k_i \prod_{j=1}^{NS} c_j^{a_j^1} \qquad (25)$$

where a_j^1 is the order of the ith reaction with respect to the jth species.

$$C_j = \frac{F_j}{\sum_{j=1}^{NS} F_j} \frac{p_t}{RT} \qquad (26)$$

The heat of reaction is the algebraic sum of the heats of formation of reactants and products:

$$-\Delta H_i = -\sum_{j=1}^{NS} \alpha_{ij} H_{fj} \qquad i = 1, NR \qquad (27)$$

where

$$H_{fj} = H_{fj}^{o} + \int_{T_{ref}}^{T} C_{pj}\, dT \qquad j=1,NS \qquad (28)$$

The boundary conditions for equations (23) and (24) are

at z=0 $F_j = F_{jo}$ j=1, NS

$T = T_{in}$

e. Method of Solution

The kinetic scheme of Mihail et al. (1983b) leads to a set of continuity equations for the reacting components that are mathematically stiff in nature because of the orders of magnitude of difference between the concentrations of molecular and ionic species. Ordinary numerical integration routines like the Runge-Kutta method fail to work for systems of stiff differential equations. A more detailed discussion on stiff differential equations can be found in the book by Davis (1984). Recently, numerical integration routines for sets of stiff differential equations have been worked out (Gear (1971)). For the purposes of integrating the above set of model equations, a code available at the University of Pittsburgh Computing Center (Hindmarsh)for solving systems of stiff differential equations (MTH:DLSODE) was used.

f. Parameter Estimation

On examining the model equations (23) and (24), it is apparent that the following parameters need to be known to perform the simulation:

Kinetic parameters - k,E

Physico-chemical parameters - C_{pj}, H_{fjo}

Operating parameters - d_t, T_{in}, F_{jo}, L

The kinetic parameters are obtained from Mihail et al. (1983b) and they are listed in Appendix I-A. The physico-chemical parameters C_{pj} and H^o_{fjo} are obtained from the property data bank in Reid et al. (1977). In those cases,

where the compounds are not listed, the parameters C_{pj} and H^{o}_{fjo} are calculated by group contribution methods.

The heat capacity C_p was calculated by the method of Rihani and Doraiswamy (1965). This method is based on the equation

$$C_p^o = \sum_i n_i a_i + \sum_i n_i b_i T + \sum_i n_i C_i T^2 + \sum_i n_i d_i T^3$$

where n_i represents the number of groups of type i. The parameters a_i, b_i, c_i and d_i are group contribution parameters.

Example: 1,5 hexadiene contains 2 $-\overset{H}{\underset{|}{C}} = CH_2$ and 2 - $\overset{|}{C}H_2$ groups.

Group i	n_i	a_i	$b_i x 10^2$	$c_i x 10^4$	$d_i x 10^6$
$-\overset{H}{\underset{|}{C}} = CH_2$	2	0.2773	3.4580	-0.1918	0.004130
$-\overset{|}{C}H_2$	2	0.3945	2.1363	-0.1197	0.002596

Thus, $C_p^{\circ} = 1.3436 + 11.1886 \times 10^{-2} T - 0.623 \times 10^{-4} T^2 + 0.013452 \times 10^{-6} T^3$ for 1,5-hexadiene.

The heat of formation at standard conditions $H^{o}_{f,298}$ is calculated by the method of Verma and Doraiswamy (1965).

Example: 1,5 hexadiene

$H^{o}_{f,298}$ = 2 (group contribution due to $C = CH_2^{H}$) + 2 (group contribution due to CH_2

= 2 x 15.02 + 2 (-4.94)

= 20.16 kcal/gmole

The parameters C_{pj} and H^{o}_{fjo} obtained from the property data bank in Reid et al. (1977) and calculated by the above group contribution methods are listed in Appendix I-A-9.

Case Study

The fixed bed reactor simulation was first performed for the case of no recycle gas and for a fixed bed microreactor which was essentially an isothermal reactor (Chang et al. (1978)). The following table shows the comparison between the experimental and predicted results.

Table I-A-9 Comparison of Experimental and Predicted Results for Fixed Bed Reactor T = 644.26, P = 1 atm WHSV = 1.0

	Experimental	Predicted
Conversion, %	99	100
Hydrocarbon Distribution, wt%		
Methane & Ethane	1.0	19.50
Propane	8.7	8.0
n-Butane + Isobutane	21.9	4.80
C_2-C_4 Olefins	1.7	24.7
C_{5+} Nonaromatics	30.5	0.8
Aromatics		
A_6-A_{10}	35.7	23.4
A_{11+}	0.5	10.70

Although the conversions are correctly predicted, the product distributions for the two cases are completely different. The total aromatic distribution

is somewhat in agreement, but the non-aromatic distributions are totally different. As was seen in the case of the fluidized bed reactor as well, the discrepancy is mainly due to the differing SiO_2/Al_2O_3 ratios in the two catalysts. A similar observation regarding product selectivity has been made by Zhang and Ou (1984). Typical concentration profiles along the length of the reactor are shown in Figures I-A-6 and I-A-7.

For the case of the actual PDU, a dehydration reactor was used in conjunction with the MTG reactor and light gases were recycled to reduce the rise in temperature. As noted by Yurchak et al.(1979), the composition of the recycle gas changed during the cycle. A typical recycle gas composition for purposes of simulation is as follows:

Methane	40 mol%
Hydrogen	10 mol%
Carbon Monoxide	10 mol%
Ethylene	10 mol%
Ethane	10 mol%
Propylene	10 mol%
Propane	10 mol%

A comparison of experimental and predicted results is shown in the following table.

Table I-A-10 Experimental and Predicted Results for PDU

	Experimental	Predicted
Outlet temperature from dehydration reactor (K)	683.71	696.04
Outlet temperature from MTG reactor (K)	723.26	741.99
Conversion (%)	100	99.8

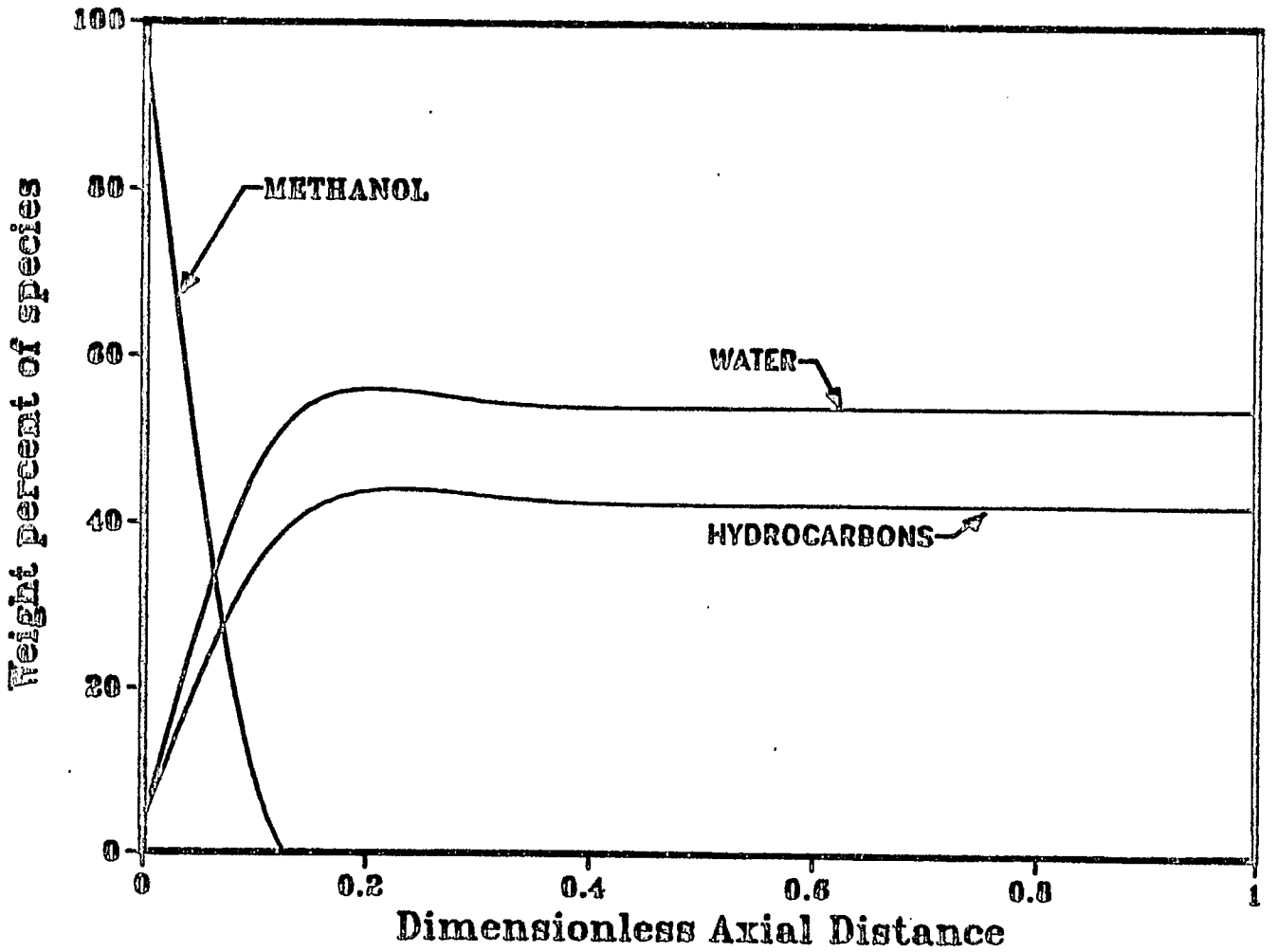

Figure I-A-6: Concentration profiles of reactant and products in fixed bed reactor (single pass, WHSV = 0.8, P = 1 atm, T = 644.26K).

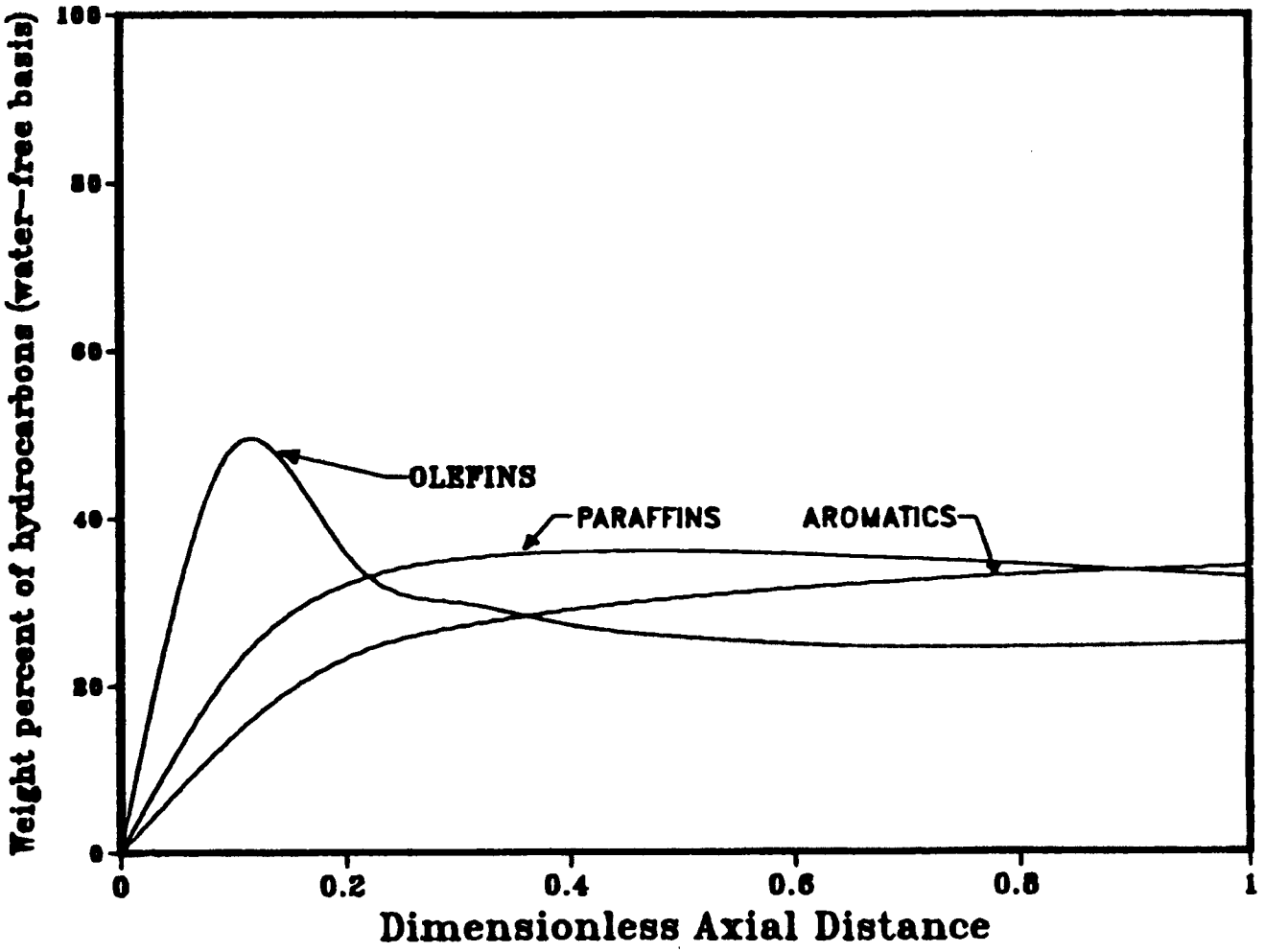

Figure I-A-7: Product distribution of hydrocarbons in fixed bed (same conditions as in Figure I-A-6).

by Mihail et al. (1983b) had a SiO_2/Al_2O_3 ratio greater than 20 (no specific number is mentioned). Hence, comparisons of the selectivities on the basis of the lumped and detailed kinetic models cannot be made with any certainty due to the differing SiO_2/Al_2O_3 ratios.

Thus, a comparison of the two reactor models is made on the basis of the lumped kinetic model of Chang et al. (1984). The following factors are considered in the comparison:

i) The same WHSV (Weight Hourly Space Velocity) is maintained in both reactors. WHSV is defined as

$$\text{WHSV} = \frac{\text{Inlet flow of reactant (kg/hr)}}{\text{weight of catalyst (kg)}}$$

Identical WHSV's can be obtained in both reactors by simultaneously changing the inlet flow and the weight of catalyst. A sound basis for comparison then suggests that the weight of catalyst in both reactors be kept constant (but not necessarily the same) and changes in WHSV be effected by changing the inlet flow of reactant. The weights of catalyst used in the two reactors are those used in the pilot plant studies of Voltz and Wise (1976) and Kam and Lee (1978). The implication of this assumption is that the geometrical dimensions of the two reactors are different.

Weight of catalyst in fluid bed = 16027 gm

Weight of catalyst in fixed bed = 132 gm

ii) Isothermal operation is assumed in both reactors. This is a reasonable assumption for the fluidized bed reactor. Though the fixed bed reactor is operated in an adiabatic manner, the use of the lumped kinetic

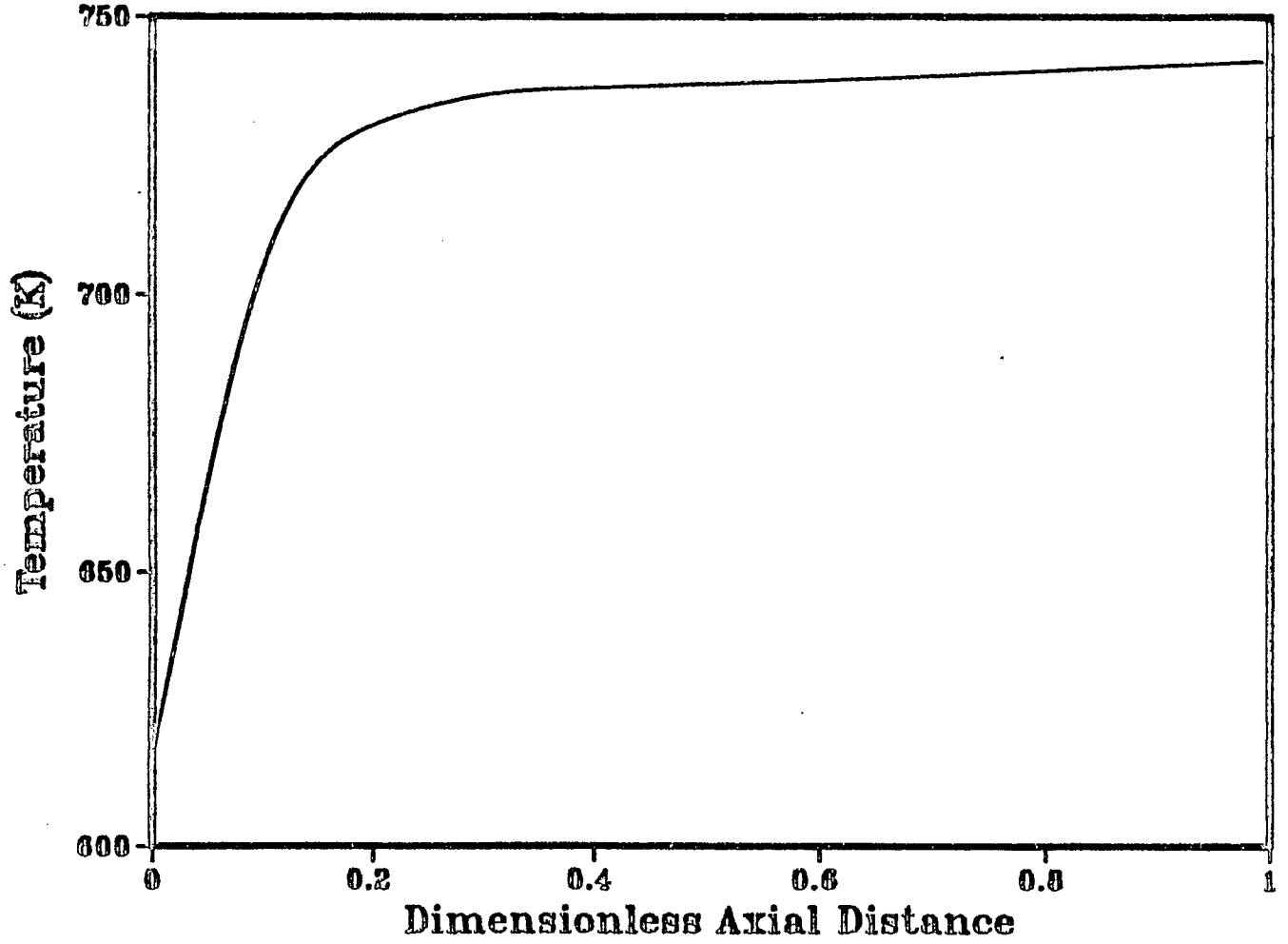

Figure I-A-8: Temperature profile in fixed bed reactor (recycle gas ratio 3.3, WHSV = 3.3, P = 19 atm).

model precludes the use of a heat balance equation in the model equations, and hence an isothermal mode of operation is adopted for the fixed bed reactor as well.

iii) The inlet temperature and pressure are the same for both reactors and there is no recycle stream for either reactor.

With the above constraints, the conversion of methanol, selectivity and space time yield (STY) are determined as a function of WHSV for the two reactors. STY is defined as follows:

$$STY = \frac{\text{moles methanol converted/time}}{\text{kg catalyst}}$$

The conversion and selectivity as a function of WHSV are shown in Figures I-A-9 and I-A-10. The decrease in conversion is much more rapid in the case of the fluidized bed reactor. The fixed bed reactor is a plug flow reactor and the decrease in conversion with WHSV is due to the decrease in space time. For the fluid bed, as WHSV increases, the portion of the gas passing through the bed as bubbles increases and a decreased efficiency of contact of reactant with the catalyst particles results since the exchange coefficient between bubble and cloud-wake remains unchanged in this case. Hence, the drop in conversion is more marked in the case of a fluid bed. Figure I-A-11 shows the selectivity to B(olefins) as a function of methanol conversion. The selectivity to B decreases with conversion for both reactors. However, for any given conversion, the selectivity to B in a fluid bed is less than that in a fixed bed. It should be noted that the fixed bed reactor model assumed no mass or heat transfer resistances or pore diffusion effects. The performance of the fluidized bed as regards the selectivity to the intermediate product, B(olefins), is typical for reactions occurring in series (Levenspiel et al.

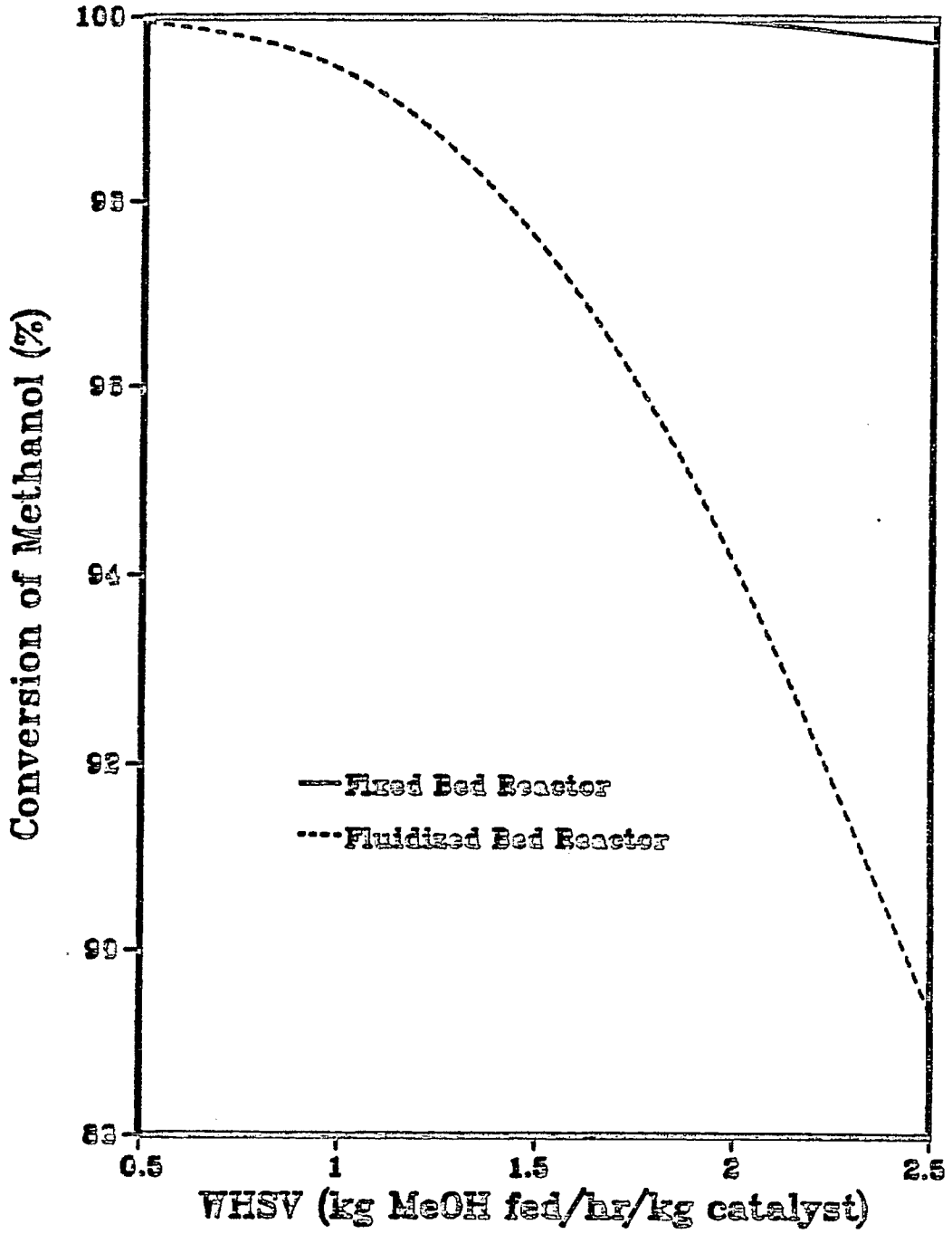

Figure I-A-9: Conversion as a function of WHSV for fixed and fluidized bed reactors. (P = 2 atm, T = 673K).

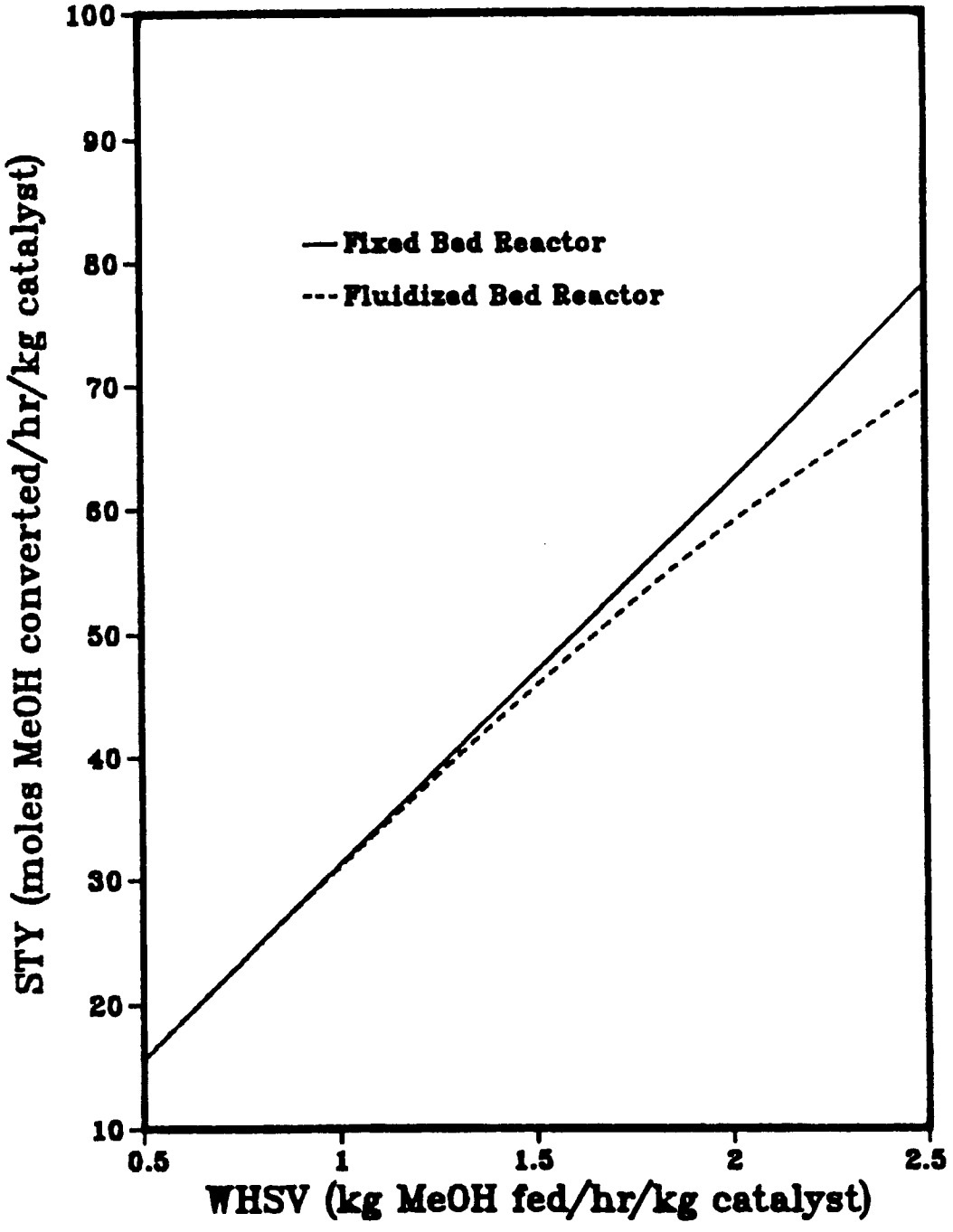

Figure I-A-10: STY as a function of WHSV for fixed and fluidized bed reactors (P = 2 atm, T = 673K).

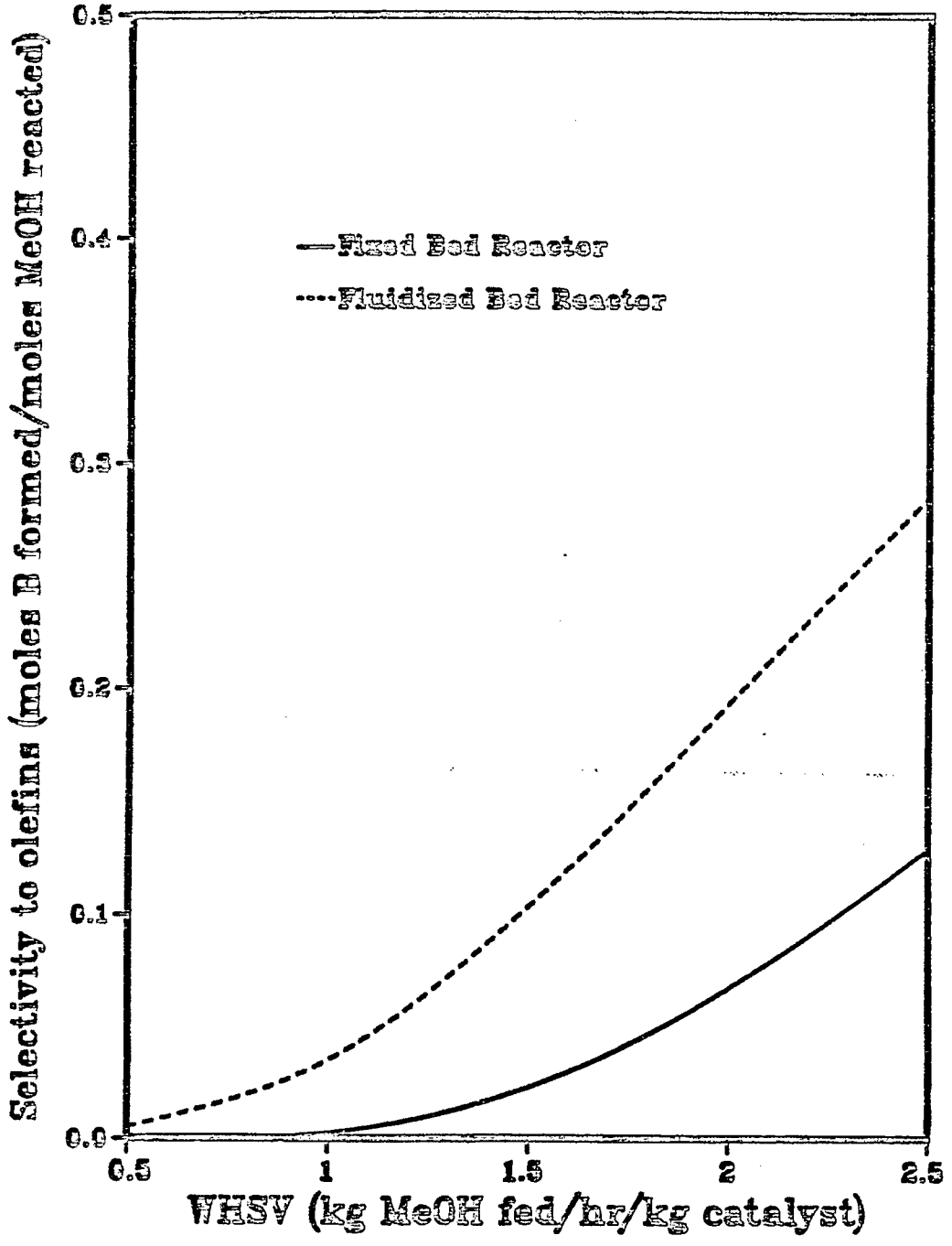

Figure I-A-11: Selectivity to olefins in fixed and fluidized bed reactors as a function of WHSV (P = 2 atm, T = 673K).

(1978)). The STY as a function of WHSV is shown in Figure I-A-12 and it can be seen that with increasing space velocity the STY for the fluidized bed is less than that for the fixed bed. This is due to the increased by-passing of gas in the form of bubbles resulting in a decrease in conversion. One way of avoiding this situation is to decrease the bubble size by introducing internals into the fluid bed which would help in breaking up the large bubbles. Factors such as conversion and selectivity are not the only considerations in the selection of a reactor. Since the MTG reaction is such a highly exothermic one, reaction heat management is a principal consideration. Some of the advantages the fluidized bed reactor has over the fixed bed reactor in this regard are (Yates (1983)):

(a) Solid particles are in continuous motion and are normally very well mixed, hence "hot spots" are rapidly dissipated and the bed operates in an essentially isothermal manner.

(b) Due to the very high bed-to-surface heat transfer that can be achieved, again as a result of particle motion, temperature control is seldom a problem.

(c) The fluid-like properties of the gas-solid mixture enable the solids to be transferred without difficulty from one vessel to another. Hence, the catalyst can be regenerated without taking the reactor off-stream, as would be the case for a fixed bed reactor.

Offsetting the above advantages are some disadvantages that in some cases are so severe that fluidized bed reactors cannot be used. These are:

(a) Erosion of bed internals, heat transfer coils, valves, etc. caused by the "sand blasting" action of the solids.

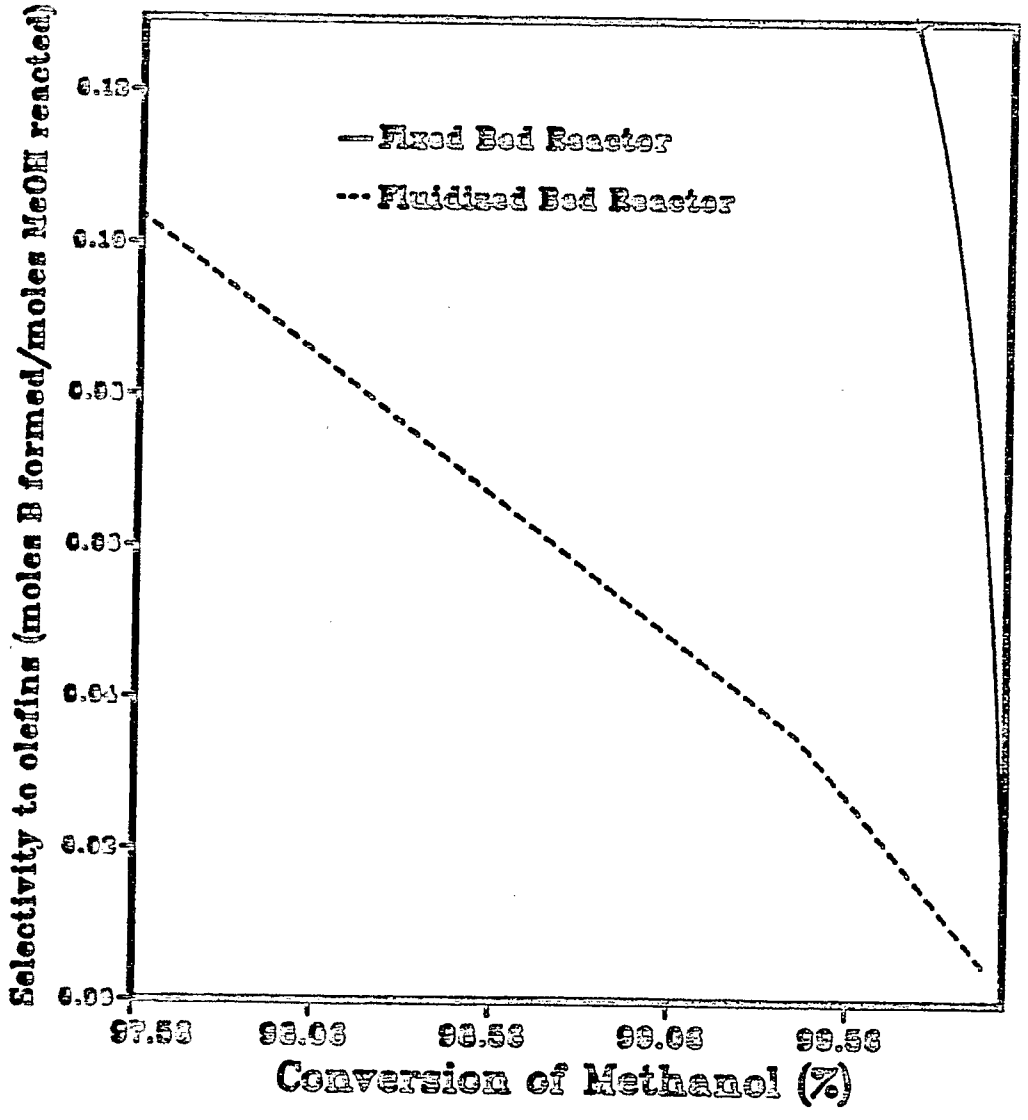

Figure I-A-12: Selectivity to olefins as a function of methanol conversion in fixed and fluidized beds (P = 2 atm, T = 673K).

(b) Loss of very fine particles through cyclone plugging and attrition. However, Mobil has claimed that it has developed a material which is not very susceptible to attrition (Haggin (1985)).

(c) By-passing of the solid by gas bubbles which can severely limit the conversion on a once-through basis.

(d) Reliable scale-up is difficult to achieve due to the limited understanding of the physics of fluidization. In fact, due to this reason Mobil decided to offer only their fixed bed reactor concept to New Zealand and carry out pilot plant studies in a 100 BPD plant before licensing the fluidized bed reactor concept (Penick et al. (1983)).

Conclusions

Modeling of the fluidized and fixed bed reactiors for the MTG process was performed in this study. The countercurrent backmixing model of Fryer and Potter (1972) was used to model the fluidized bed, while the one-dimensional pseudo-homogeneous model was used for the fixed bed. Model predictions for methanol conversion compared well with experimental conversions. However, product selectivities from the model simulations were not in good agreement with experimental results. This was mainly due to the fact that the SiO_2/Al_2O_3 ratio in the 2SM-5 catalyst used in the pilot plant studies has not not been reported. The SiO_2/Al_2O_3 ratio in the 2SM-5 catalyst has a major influence in determining product selectivity. Thus, a knowledge of the SiO_2/Al_2O_3 ratio is essential for correctly predicting product selectivities. A comparison of the fixed and fluidized bed reactors for the MTG process was done on both a quantitative and qualitative basis. This comparison revealed that though the fixed bed reactor gave high conversion and a higher selectivity to intermediate product (olefins) at a given WHSV as

compared to the fluidized bed, the fluidized bed reactor was better in terms of reaction heat management.

Nomenclature:

C_B	reactant concentration in bubble gas, moles/cc
C_C	reactant concentration in cloud-wake gas, moles/cc
C_H	reactant concentration in exit gas, moles/cc
C_{pj}	specific heat of component j, kcal/kmol.K
C_P	reactant concentration in particulate phase gas, moles/cc
C_i	reactant concentration in inlet gas, moles/cc
d_t	reactor diameter, m
D_B	diameter of sphere having the bubble volume, cm
D_G	gas phase diffusion coefficient, cm^2/sec
f_w	ratio of wake volume to bubble volume
F_j	molar feed rate of species j, kmol/s
g	gravitational acceleration, cm/sec^2
F_{jo}	inlet molar feed rate of species j, kmol/s
H	height of bubbling bed, cm
H_{fj}	heat of formation of species j, kcal/kmol
H^o_{fj}	heat of formation of species j, kcal/kmol
$-\Delta H_i$	heat of reaction for reaction i, kcal/kmol
H_{mf}	height of fluidized bed at minimum fluidizing conditions, cm
k, k_1, k_2	first order reaction rate constants, sec^{-1}
K_{BC}	volumetric rate of gas exchange between bubble and cloud-wake per unit bubble volume, sec^{-1}
K_{CP}	volumetric rate of gas exchange between cloud-wake and particulate phase per unit bubble volume, sec^{-1}
p_t	operating pressure, atm
q(z)	heat removal per unit length of reactor, kcal/m.s
r_i	rate of reaction per unit volume, $kmol/m^3s$
R	gas constant, m^3 atm/kmol K
R_j	total rate of change of the amount of component j, kmol/m3s

T	temperature, K
T_{in}	inlet temperature to reactor, K
u_a	bubble rise velocity, cm/sec
U	superficial velocity of fluidizing gas, cm/sec
U_{cr}	superficial gas velocity above which backmixing occurs, cm/sec
U_{GB}	superficial gas velocity in bubble phase, cm/sec
U_{GC}	superficial gas velocity in cloud-wake region, cm/sec
U_{GP}	superficial gas velocity in cloud-wake region cm/sec
U_{mf}	superficial gas velocity at incipient fluidization, cm/sec
z	distance along reactor, m

Greek Letters

α_{ij}	stoichiometric coefficient of component j with respect to the ith reaction
ε_B	fraction of bed volume occupied by bubbles
ε_{mf}	voidage fraction at incipient fluidization

References

Anthony, R.G., "A Kinetic Model for Methanol Conversion to Hydrocarbons", Chem. Eng. Sci., 36, 789 (1981).

Ascher, U., J. Christiansen and R.D. Russel, "Collocation Software for Boundary-Value ODE's", ACM Trans. on Math. Software, 7 (2), 209 (1981).

Chang, C.D., Hydrocarbons from Methanol, Marcel Dekker Inc., New York (1983).

Chang, C.D., "A Kinetic Model for Methanol Conversion to Hydrocarbons", Chem. Eng. Sci. 35, 619 (1980).

Chang, C.D. and A.J. Silvestri, "The Conversion of Methanol and Other O-compounds to Hydrocarbons over Zeolite Catalysts", J. Catal., 47, 249 (1977).

Chang, C.D., J.C.W. Kuo, W.H. Lang, S.M. Jacob, J.J. Wise and A.J. Silvestri, "Process Studies on the Conversion of Methanol to Gasoline," Ind. Eng. Chem. Process Des. Dev. 17, 255 (1978).

Chang, C.D., C.T.W. Chu and R.F. Socha, "Methanol Conversion to Olefins over ZSM-5 I. Effect of Temperature and Zeolite SiO_2/Al_2O_3", J. Catal., 86, 289 (1984).

Davis, M.E., Numerical Methods and Modeling for Chemical Engineers, John Wiley & Sons, New York, (1984).

Chen, N.Y. and W.J. Reagan, "Evidence of Autocatalysis in Methanol to Hydrocarbon Reactions Over Zeolite Catalysts", J. Catal., 59, 123 (1979).

Flatow, D., N. Daviduk and H. Heiart, "Conversion of Methanol to Gasoline, Engineering and Construction of the Demonstration Plant", DOE Report No. DOE/NBM-500323, March (1984).

Froment, G.F. and K.B. Bischoff, Chemical Reactor Analysis and Design, John Wiley & Sons, New York (1979).

Fryer, C. and O.E. Potter, "Countercurrent Backmixing Model for Fluidized Bed Catalytic Reactors. Applicability of Simplified Solutions", Ind. Eng. Chem. Fundam., 11 (3), 338 (1972).

Gear, C.W., Numerical-Initial Value Problems in Ordinary Differential Equations, Prentice-Hall, Englewood Cliffs, N.J. (1971).

Haggin, J., "First Methanol-to-Gasoline Plant Nears Startup in New Zealand", Chem. and Eng. News, March 25, 1985, p. 39.

Hindmarsh, A., Mathematical and Statistical Division, Lawrence Livermore Laboratories.

Kam, A.Y. and W. Lee, "Fluid Bed Process Studies on Selective Conversion of Methanol to High Octane Gasoline", DOE Report No. FE-2490-15, April (1978).

Kikuchi, E., S. Hatanaka, R. Hamana, and Y. Morita, "The Acidic Properties of ZSM-5 Zeolite and its Catalytic Activity in the Conversion of Methanol", Int. Chem. Eng., 24 (1), 146, (1984).

Kunii, D. and O. Levenspiel, "Bubbling Bed Model. Model for the Flow of Gas Through a Fluidized Bed", Ind. Eng. Chem. Fundam., 7, 446 (1968a).

Kunii, D. and O. Levenspiel, "Bubbling Bed Model for Kinetic Processes in Fluidized Bed. Gas-Solid Mass and Heat Transfer and Catalytic Reaction," Ind. Eng. Chem. Process Des. Dev., 7, 481 (1968b).

Levenspiel, O., N. Baden and B.D. Kulkarni, "Complex First-Order Reactions in Fluidized Reactors: Application of the KL Model", Ind. Eng. Chem. Process Des. Dev. 17, 478 (1978).

Liederman, D., S.M. Jacob, S.E. Voltz and J.J. Wise, "Process Variable Effects in the Conversion of Methanol to Gasoline in a Fluid Bed Reactor," Ind. Eng. Chem. Process Des. Dev. 17, 340 (1978).

Meisel, S.L., J.P. McCullough, C.H. Lechthaler and P.B. Weisz, "Gasoline from Methanol in One Step", Chem. Tech. February, 86 (1976).

Mihail, R., S. Straja, Gh. Moria, G. Musca and Gr. Pop, "Kinetic Model for Methanol Conversion to Olefins" Ind. Eng. Chem. Process Des. Dev., 22 (3), 532 (1983a).

Mihail, R., S. Straja, Gh. Moria, G. Musca and Gr. Pop., "A Kinetic Model for Methanol Conversion to Hydrocarbons" Chem. Eng. Sci., 38, 1581 (1983b).

Penick, J.E., W. Lee and J. Maziuk, "Development of the Methanol-to-Gasoline Process" in Chemical Reaction Engineering-Plenary Lectures (J. Wei and C. Georgakis eds.) ACS Symposium Series No. 226, 19 (1983).

Raghuraman, J. and O.E. Potter, "Countercurrent Backmixing Model for Slugging Fluidized-Bed Reactors," AIChE J. 24, 698 (1978).

Reid, R.C., J.M. Prausnitz and T.K. Sherwood, The Properties of Gases and Liquids, McGraw-Hill, New York (1977).

Rihani, D.N. and L.K. Doraiswamy, "Estimation of Heat Capacity of Organic Compounds from Group Contributions", Ind. Eng. Chem. Fundam., 4, 17 (1965).

Stewart, P.S.B. and J.F. Davidson, "Slug Flow in Fluidized Beds", Powder Tech., 1, 61 (1967).

Swabb, E.A. and B.C. Gates, "Diffusion, Reaction and Fouling in H-Mordenite Crystallites. The Catalytic Dehydration of Methanol", Ind. Eng. Chem. Fundam., 11, 541 (1972).

Verma, K.K. and L.K. Doraiswamy, "Estimation of Heats of Formation of Organic Compounds", Ind. Eng. Chem. Fundam., 4, 389 (1965).

Voltz, S.E. and J.S. Wise, "Development Studies on Conversion of Methanol and Related Oxygenates to Gasolines", Final Report, prepared for ERDA under Contract No. E(49-18)-1773, November (1976).

Yates, J.G., Fundamentals of Fluidized-Bed Chemical Processes, Butterworths, London (1983).

Yates, J.G. and J.Y. Gregoire, "Catalytic Oxidation of O-Xylene in a Slugging Fluidized Bed," Chem. Eng. Sci. 35, 380 (1980).

Yurchak, S., S.E. Voltz and J.P. Warner, "Process Aging Studies in the Conversion of Methanol to Gasoline in a Fixed Bed Reactor", Ind. Eng. Chem. Process Des. Dev., 18, 527 (1979).

Zhang, Z. and G. Ou, "Investigation and Evaluation of a Methanol-to-Hydrocarbon Catalyst in a Laboratory Scale Reactor", Int. Chem. Eng., 24, 368 (1984).